

THE INFLUENCE OF TELECONNECTIONS ON THE  
PRESENCE OF NORTH ATLANTIC ICEBERGS  
SOUTH OF 48°N: 1983-2020

by

Shayne R. O'Brien, B.A, M.S

A dissertation submitted to the Graduate Council of  
Texas State University in partial fulfillment  
of the requirements for the degree of  
Doctor of Philosophy  
with a Major in Geography  
December 2022

Committee Members:

Richard W. Dixon, Chair

Yanan Li

Nathan Allen Currit

Todd W. Moore

**COPYRIGHT**

by

Shayne R. O'Brien

2022

## **FAIR USE AND AUTHOR'S PERMISSION STATEMENT**

### **Fair Use**

This work is protected by the Copyright Laws of the United States (Public Law 94-553, section 107). Consistent with fair use as defined in the Copyright Laws, brief quotations from this material are allowed with proper acknowledgment. Use of this material for financial gain without the author's express written permission is not allowed.

### **Duplication Permission**

As the copyright holder of this work I, Shayne R. O'Brien, authorize duplication of this work, in whole or in part, for educational or scholarly purposes only.

## **DEDICATION**

This document is dedicated to my wife Elizabeth.

Without her, it would not exist.

## **ACKNOWLEDGEMENTS**

I would like to extend thanks to my advisor, Dr. Richard Dixon for his mentorship in completing this document, and throughout my program. Thank you to my Committee, Dr. Nathan Currit, Dr. Yanan Li, and Dr. Todd Moore for their personal and professional guidance. Mike Hicks, Chief Scientist for the International Ice Patrol was also instrumental in conducting this research.

## TABLE OF CONTENTS

	<b>Page</b>
ACKNOWLEDGEMENTS .....	v
LIST OF TABLES.....	viii
LIST OF FIGURES .....	ix
LIST OF ACRONYMS .....	xi
ABSTRACT .....	xii
CHAPTER	
1. INTRODUCTION .....	1
1.1 Overview .....	1
1.2 Purpose Statement .....	2
1.3 Research Objectives.....	3
1.4 Chapter One Tables.....	6
2. LITERATURE REVIEW .....	7
2.1 Teleconnections.....	7
2.2 The International Ice Patrol .....	9
2.3 Atlantic Multidecadal Oscillation.....	11
2.4 Ocean-Ice-Atmosphere Interactions on the Greenland Ice Sheet .....	11
2.5 Iceberg Production and Transit .....	12
3. RESEARCH METHODS .....	14
3.1 Study Site.....	14
3.2 Methods and Data Analysis .....	15
4. RESULTS .....	22
4.1 Iceberg Lag Times Through Use of Linear Regression Modeling .....	22
4.2 Logistic Regression Modeling Iceberg Count Based on NAO/AO .....	23
4.3 Model Fit Based on Akaike’s Information Criterion .....	23
4.4 NAO/AO as a Driver of Sea Ice Extent.....	24

4.5 Sea Ice Maximum as a Driver of I48N's.....	24
4.6 Case Studies.....	25
4.7 Chapter Four Figures.....	33
5. DISCUSSION.....	64
5.1 Discussion of Lag Models.....	64
5.2 Discussion of Logistic Regression Modeling.....	64
5.3 Discussion of AIC Testing of Model Fit.....	66
5.4 NAO/AO as a Driver of Sea Ice Extent.....	67
5.5 Sea Ice Maximum as a Driver of I48N's.....	68
5.6 Discussion of Case Studies.....	69
6. CONCLUSION.....	71
6.1 Summary.....	71
6.2 Future Research.....	73
6.3 Concluding Statement.....	75
APPENDIX I: MONTHLY ICEBERG COUNTS 1983-2020 (G10028).....	76
APPENDIX II: LOGISTIC REGRESSION BINARY VARIABLES.....	77
LITERATURE CITED.....	78

## LIST OF TABLES

<b>Table</b>	<b>Page</b>
1.1: List of reanalysis model variables to be included in case studies.....	6
4.1: Linear Regressions, North Atlantic Oscillation.....	57
4.2: Linear Regressions, Arctic Oscillation.....	58
4.3: Logistic Regressions .....	59
4.4: AIC Testing .....	60
4.5: Linear Regressions, NAO v. Sea Ice.....	61
4.6: Linear Regressions, AO v. Sea Ice .....	62
4.7: Linear Regressions, Sea Ice v. I48Ns.....	63

## LIST OF FIGURES

<b>Figure</b>	<b>Page</b>
4.1(a) AO/NAO v. I48Ns (0-Year Lag) .....	33
4.1(b) AO/NAO v. I48Ns (1-Year Lag) .....	34
4.1(c) AO/NAO v. I48Ns (2-Year Lag) .....	35
4.1(d) AO/NAO v. I48Ns (3-Year Lag) .....	36
4.2(a) Logistic Regression, North Atlantic Oscillation .....	37
4.2(b) Logistic Regression, Arctic Oscillation .....	38
4.2(c) Logistic Regression, AO and NAO .....	39
4.3(a) AO/NAO v Maximum Sea Ice Concentration (0-Year Lag) .....	40
4.3(b) AO/NAO v Maximum Sea Ice Concentration (1-Year Lag) .....	41
4.3(c) AO/NAO v Maximum Sea Ice Concentration (2-Year Lag) .....	42
4.3(d) AO/NAO v Maximum Sea Ice Concentration (3-Year Lag) .....	43
4.4 (a) Sea Ice Maximum v. I48Ns (0-Year Lag) .....	44
4.4 (b) Sea Ice Maximum v. I48Ns (1-Year Lag) .....	45
4.4 (c) Sea Ice Maximum v. I48Ns (2-Year Lag) .....	46
4.4 (d) Sea Ice Maximum v. I48Ns (3-Year Lag) .....	47
4.6.1 Reanalysis, Geopotential Height .....	48
4.6.2 Reanalysis, Relative Humidity .....	49
4.6.3 Reanalysis, Omega .....	50
4.6.4 Reanalysis, Sea Ice .....	51
4.6.5 Reanalysis, Sea Level Pressure .....	52

<b>Figure</b>	<b>Page</b>
4.6.6 Reanalysis, SST/Skin Temperature .....	53
4.6.7 Reanalysis, Air Temperature .....	54
4.6.8 Reanalysis, Zonal Wind.....	55
4.6.9 Reanalysis, Meridional Wind .....	56

## LIST OF ACRONYMS

- AIC – Akaike Information Criterion
- AMIP-II – Atmospheric Model Intercomparison Project II
- AO – Arctic Oscillation
- AOI – Arctic Oscillation Index
- DOE – Department of Energy
- EOF – Empirical Orthogonal Function
- GrIS – Greenland Ice Sheet
- I48N – Iceberg observed south of 48°N
- IIP – International Ice Patrol
- NAO- North Atlantic Oscillation
- NAOI- North Atlantic Oscillation Index
- NASA – National Aeronautics and Space Administration
- NCAR – National Center for Atmospheric Research
- NCEP – National Centers for Environmental Protection
- PC – Principal Component
- RMS – Royal Mail Ship
- SLAR – Side-Looking Aperture Radar
- SMB – Surface Mass Balance
- SST – Sea Surface Temperature
- USCG – United States Coast Guard

## **ABSTRACT**

The International Ice Patrol (IIP) has been responsible for the safety of maritime activity related to icebergs in the North Atlantic since their founding in the wake of the Titanic disaster in April 1912. In the century to follow, the Ice Patrol, their mission, methods, and technology have evolved. Today, a century of iceberg observation data collected by the IIP has led to a growing field of climatological and hazards sciences related study. This study examines the North Atlantic Oscillation (NAO) and Arctic Oscillation (AO) as drivers of iceberg presence south of 48°N through direct and secondary influence between 1983 and 2020. This study is divided into five sections which examine different aspects of the relationship between teleconnections and icebergs south of 48°N (I48N). The first section identifies that the NAO and AO have statistically significant correlation with the number of I48Ns at a 1-year lag, through the use of linear regression modelling. The second section determines through the use of logistic regression that there is a statistically significant increase likelihood of an Extreme (>1399) iceberg year in years following a high annual NAO Index. Section three includes the comparison of AIC values for different AO/NAO models, which concluded that NAO is a stronger driver of North Atlantic icebergs than the AO. Section four involves a twofold analysis of the role of sea ice in iceberg-teleconnection interactions. These analyses resulted in the finding that sea ice has a significant correlation with I48N counts at 0- and 1-year lags. Additionally, this section indicates a significant correlation between sea ice and AO at a 1-year lag. Section five consists of comparing reanalysis(NCEP/NCAR Reanalysis, NCEP/DOE R2) data of meteorological and

oceanographic factors in the 3 most-recent high and low iceberg years. This comparison identified areas of future study including geopotential height, sea level pressure and sea surface temperature.

# 1. INTRODUCTION

## 1.1 Overview

On the 14<sup>th</sup> of April 1912, at 11:40pm EST the British passenger ship RMS Titanic struck an iceberg at approximately 41°43' N, 49°56' W, (370 miles south-southwest of Newfoundland) on her maiden voyage from Southampton, UK to New York, NY. The ship would sink over the next three hours, with a loss of life of more than 1,500. The sinking of the Titanic provided the impetus for the international community to address a lack of official iceberg information available to trans-Atlantic mariners. Therefore, in 1914 the International Ice Patrol (IIP) was created, to be undertaken by the United States Coast Guard. In the century since the humble beginnings of the IIP, the modern IIP collects iceberg data from aircraft equipped with side-looking aerial radar (SLAR), and reports iceberg conditions in the North Atlantic twice daily. The IIP's mission of safeguard lives in the North Atlantic from the threat of icebergs has had the added side-effect of creating a long-term dataset of Iceberg observations in the North Atlantic south of 48° N.

The International Ice Patrol has historically defined an ice year (October through September) with more than 600 icebergs observed as an extreme year (IIP, 1994). In the time since the IIP began collecting data using SLAR (1983), more than 60% percent of annual observations have been considered extreme. With an average annual iceberg observation between 1983 and 2016 of 787, compared to an average of 487 icebergs observed annually between 1900 and 2015. However, in 2018, research conducted by the IIP concluded that much of the variation between reconnaissance periods can be explained by changes in observation technology (Rudnickas and Serumgard, 2018). The IIP introduced normalized iceberg data from 1900 – 2018 and created new season severity guidelines based on a normal distribution, creating a new threshold of extreme for the period of 1983 – 2020

as  $\geq 1399$  icebergs. Considering the lack of a positive trend in icebergs south of  $48^\circ$  N in either dataset, the question of the causes of interannual and interdecadal variability arises. Increasing interannual variability is found regularly in the data after ice year 1968 (October 1967 – September 1968) (IIP, 2018).

The presence of icebergs south of  $48^\circ$ N (I48N) is largely reliant on increased iceberg calving due to mass balance loss on the Greenland Ice Sheet (GrIS) (Bigg, 1999, Howat et al., 2010, Bigg et al., 2014). As well as sea surface temperatures (SST) in the Labrador Sea (Yashayaev, 2007), and Labrador current vector (Palter et al. 2016). Given the focus on the influence of iceberg calving in Western Greenland coastal outlet glaciers, it becomes apparent that the influence that teleconnections such as the North Atlantic Oscillation (NAO) and Arctic Oscillation (AO) have on GrIS Surface mass balance (SMB) is key to quantifying the role that the NAO and AO have on the presence of I48N.

Additionally, the NAO Index (NAOI) is known to influence sea ice development off of Labrador and Newfoundland. Positive phases of the NAOI deliver cold winds to coastal areas of Labrador and Newfoundland, which lead to increased sea ice development that prevents grounding events of icebergs (IIP, 2016; IIP 2018) and allows icebergs to continue their southward travel. Understanding the influence each of these variables, all of which are at least in part driven by Arctic teleconnections, have on the recorded number of I48Ns annually would be especially useful in creating improved I48N forecasts.

## **1.2 Purpose Statement**

The number of Icebergs detected south of  $48^\circ$ N (I48N) have been tracked for over a century, by the IIP beginning in 1913, and the U.S Hydrographic Office prior, utilizing a wide array of observation technologies. These changing technologies have created noise in

the data that creates uncertainty when attempting temporally long-range statistics. However, with four decades of Side-Looking Aerial Radar (SLAR) observation data, a standardized climatological analysis can be performed (IIP, 2014, IIP, 2018).

With the portion global trade crossing the North Atlantic increasing the accuracy of iceberg forecasts is of paramount importance, especially in a changing climate. Preliminary research has been conducted by the IIP (Rudnickas and Serumgard, 2018) into linkages between the NAO, AO and I48Ns, and have found some links between sea ice conditions and I48Ns related to these teleconnections. Exploring these meteorological and oceanographic conditions is an essential part of creating a viable forecasting system,

The purpose of this research is to investigate the influence of the North Atlantic Oscillation and the Arctic Oscillation on presence of I48Ns, by Testing the influence of NAO and AO on the presence of I48Ns

A key development in previous research (Rudnickas and Serumgard, 2018), is that this research is not designed to explain trends such as increasing or decreasing I48N presence, it is designed to explain variability. Annual ice year I48N counts are not increasing over time, but they are becoming more variable.

### **1.3 Research Objectives**

This work is designed to achieve several objectives. First, by using statistics, identify the ideal lag time between an NAO or AO event and the I48Ns that are present in relation to them. The accepted period of iceberg transit is between 1-3 years (IIP; 2016, IIP 2018; IIP, 2020). This objective will be achieved by performing linear regressions on annual timescales between NAO and AO indices, and I48N presence to identify the lag time with

the highest correlation coefficient, and statistical significance. This information will be used as a baseline time lag.

Once the first objective is complete, a series of logistic regressions (Meyers, Gamst & Guarino, 2013) will be performed. This is designed to identify the impact of NAO and AO Index on the likelihood of Light, Moderate, Heavy, and Extreme iceberg years. In understanding possible trends in ice year probability based on NAO and/or AO, additional questions arise including which teleconnection is the stronger influence, and how is the likelihood of each iceberg severity category impacted by these teleconnections? This test will be performed with a significance level of 0.05.

Following the logistic regressions, Akaike's Information Criterion (AIC) (Akaike, 1973) of a variety of teleconnection regression models will be calculated and compared, in order to identify whether NAO or AO is the stronger direct influence on I48Ns. These models will be ordered by decreasing influence of AO. (NAO Only, NAO $\times$ AO, NAO + AO, NAO-AO, NAO/AO, AO Only.). Lower AIC is indicative of a stronger model. This method will produce ranked AIC values based on strongest-to-weakest model. The order of these ranked models will determine whether NAO or AO is the stronger driver of I48Ns.

Of the possible drivers of I48Ns Sea Ice (Marko et al. 1994, Rudnickas and Serumgard 2018) comes at the recommendation of the IIP for further analysis, mostly along the Labrador Shelf of Eastern Canada. As an intermediate step between teleconnections and I48Ns, sea ice data maximum percentage data from the coastal region of Northern Labrador will be tested against both NAO and AO indices, as well as against I48Ns. This is to determine how much, and at which lags NAO and AO drive coastal sea ice, and then determine how much this sea ice impacts I48Ns.

With inferential statistics regarding the factors that lead to presence of I48Ns complete, the research moves to a more qualitative approach. Six cases studies will be created, comprising the three most recent years with the highest number of I48Ns and the three years with the lowest number of I48Ns. These case studies will include the most recent high (I48N) ice years 2014(1546), 2019(1515), 2009(1204) and low I48N ice years 2010 (1), 2011(3), and 2013 (13). These case studies will use an array of NCEP/DOE Reanalysis II (Kanamitsu et al., 2002) and NCEP/NCAR Reanalysis (Kalnay et al., 1996, Kistler et al. 2001) to examine the spatial conditions of both icebergs and other potential meteorological/oceanic drivers during these ice years.

These studies will allow for an understanding of the physical meteorology and oceanography involved in I48N presence in a given year. Physical and spatial context provided by the reanalysis data will allow for a complete picture of the events that lead to I48N presence. The reanalysis products that will be incorporated into the case studies are outlined in Table 1.1.

The overall combination of full data period statistics, and in-depth analysis of exemplary cases of I48Ns offers the unique opportunity to draw conclusions about the overall state of the North Atlantic to broadly increase understanding of I48Ns and to equip stakeholders with the ability to more accurately forecast ice year severity.

#### 1.4 Chapter One Tables

Table 1.1. List of reanalysis model variables to be included in case studies. All models are surface (1000mb) unless otherwise denoted. Models built using NCEP/DOE Reanalysis II.

Geopotential Height (500hPa)	Relative Humidity	Omega
Sea Ice	Sea Level Pressure	Skin Temperature/SST
Air Temperature	Zonal Wind	Meridional Wind

## 2. LITERATURE REVIEW

### 2.1 Teleconnections

Teleconnections are links between environmental events, climatic variations in particular, separated by time and geography that result from interconnections of the atmospheric system (Huggett, 2010). Change in one component of the atmosphere leads to changes in others, often with a temporal delay, and affecting areas great distances from the source of the original change (Huggett, 2010). Teleconnections such as the El Niño Southern Oscillation (ENSO) (Walker, 1924), North Atlantic Oscillation (NAO), and the North Pacific Oscillation (NPO) (Walker, 1928), were all discovered in the early 20<sup>th</sup> century by British statistician and physicist Sir Gilbert Walker (b.1868, d.1958).

In the Arctic, the dominant teleconnections are the North Atlantic Oscillation (NAO) and the Arctic Oscillation (AO). (Wallace and Gutzler, 1981; Huggett, 2010; Barry and Gan, 2011, Serreze and Barry, 2014). In the North Atlantic region, the NAO is the dominant winter climate variability mode, and is considered a regional manifestation of the pan-Arctic AO (Thompson and Wallace, 2000). While both the AO and NAO are present year-round, these teleconnections and the weather they influence are most prominent during the winter. (Barnston and Livezy, 1987).

The NAO exists in two phases, positive and negative, which describe covariation between the Icelandic Low and Azores High (Serreze and Barry, 2014). These pressure centers covary as mass moves between them. When the NAO is in its positive phase, both the Icelandic Low and Azores high are stronger than their mean levels, which the opposite covariation goes for the NAO when it is in its negative phase. These phases can fluctuate over periods of a few months on average, according to time series data of NAO index (Hurrell, 2020), however these monthly trends in NAO index can also average out to periods

of years where these pressure regimes are on average high or low (Walker and Bliss, 1932; Hurrell, 1995). The positive phase is characterized by a strengthening of the Azores High and Icelandic Low. When this occurs, the polar jet remains strong, and cold temperatures are kept in the Arctic (Francis and Vavrus, 2015). This phase is often aligned with the positive phase of the AO. During this phase, temperatures in Greenland and the North Atlantic remain cold, and provide conditions that are conducive to the growth of sea ice in Baffin Bay and the Labrador Sea (Walker and Bliss, 1932, Marko et al. 1994; Hurrell, 1995, Rudnickas and Serumgard, 2018). Gilbert Walker and E.W Bliss first detected strong correlation between positive NAO and North Atlantic Icebergs in 1933 (Walker and Bliss, 1937).

In contrast to the positive phase, the negative phase of the NAO occurs when both the Icelandic Low and Azores High are weaker than average (Serreze and Barry, 2014). This phase is characterized by a weaker jet (Francis and Vavrus, 2015), which increases warm air advection poleward and cold air advection equatorward. This phase increases warmth in Baffin Bay, Labrador Sea and Greenland, which in turn decreases sea ice found in this region. (Hurrell, 1995; Huggett, 2010; Barry and Gan, 2011; Serreze and Barry, 2014). Periods of negative NAO have also shown correlation with periods of extreme ice melt on the Greenland Ice Sheet by reducing snowfall and increasing summertime warming (Bevis et al., 2019).

The AO, in contrast to the NAO encompasses the entire Northern Hemisphere. The Arctic Oscillation is an annual oscillation of atmospheric mass in the northern hemisphere, between the pole, and the mid-latitudes. When this fluctuation shifts more mass to the midlatitudes, the AO is in its positive mode, while more mass in the Arctic reflects the

negative mode. This is calculated using 1000- hPa height anomalies. (Thompson and Wallace, 1998). During the positive phase of the AO, the subpolar jet is strong, much like with the NAO. This strong jet leaves colder temperatures in the North Atlantic. Additionally, the negative phase acts much in the same way as the NAO negative phase, leading to a weaker jet and more cold air advection into the midlatitudes and warm air advection into the North Atlantic and Greenland (Thompson and Wallace, 1998, Thompson and Wallace, 2000).

## **2.2 The International Ice Patrol**

Between November 23, 1913, and January 20, 1914, delegates from 13 countries held the First International Conference on the Safety of Life at Sea (SOLAS), where they signed an agreement to invite the United States to undertake an initiative to patrol the North Atlantic shipping lanes for icebergs at the expense of the 13 delegate nations, to avoid a repeat of the 1912 Titanic disaster (Wheeler, 1914). The agreement was signed by President Woodrow Wilson on March 17<sup>th</sup>, 1914. At first, this mission is undertaken by the Revenue Cutter Service, but was turned over to the United States Coast Guard (USCG) in 1915. The USCG is still in charge of the mission, which is now called the International Ice Patrol (IIP) (Smith, 1926a, Murphy and Cass, 2012). At the founding of the IIP there were two main missions, locating threatening icebergs in steamship tracks while making the information available to mariners, and making scientific observations to increase understanding of icebergs in the North Atlantic (Smith, 1926a). This second mission led to the creation of NSIDC Dataset (G10028), Record of Icebergs South of 48°N (IIP, 1995, IIP 2020). This dataset is a monthly record of ice observations beginning in October 1899.

After the hiatus in the IIP's operations caused by the First World War, Edward "Iceberg" Smith started his tenure as Director of the IIP. During this period, Smith began

the process of modernizing the IIP. After participating in the Graf Zeppelin expedition to the Arctic in 1931, Smith began to prepare for the IIP's first technological leap (Ellsworth and Smith, 1931) by the end of the Second World War, the IIP had begun conducting their ice survey completely using aircraft. This change in technology is visible in the data, as the number of icebergs sighted increased from the days of patrol boat reconnaissance (Rudnickas and Serumgard, 2018). During the airborne observation period (1945-1983) The IIP became able to scout north of their study area, allowing them to begin to observe Arctic Sea ice conditions. During this period, changes were made in the definition of an ice year. Between 1926 and 1967, an Ice Year was the calendar year, changing in 1967 to September-August. Finally, the modern Ice Year of October-September became active in 1982 for two reasons. Beginning the Ice Year in October reduced the likelihood of iceberg season carry over from the previous year, as September iceberg sightings are more likely than October, and to match the U.S Government's Fiscal year (IIP, 2011).

In 1983, the IIP began conducting observations using side-looking aperture radar (SLAR). This change caused the most recent leap in observational capability in iceberg reconnaissance, which led to a further increase in annual iceberg sightings. Based on this new metric Rudnickas and Serumgard (2018) discussed new definitions for season severity, and normalization for previous records to examine if changes in observational technology were leading to false trends in icebergs data, which they were.

### **2.3 Atlantic Multidecadal Oscillation**

The Atlantic Multidecadal Oscillation (AMO) has been believed to be the regime that includes natural fluctuations in ocean temperatures of the North Atlantic in periods of around 60-80 years and is based on average sea surface temperature (SST) anomalies (anomaly being deviation from the mean) in the North Atlantic (Mann et al, 1995; Delworth

and Mann, 2000). However, in early 2021, new research from Mann and others (2021) suggested that when removing post-industrial anthropogenic and volcanic forcings from coupled earth-ocean-atmosphere models, there is not a natural temperature fluctuation indicated. While Mann and others (2021) has presented this updated AMO research as definitive, there is some uncertainty raised regarding the study's reliance on computer modeling. There is yet to be a published rebuttal on the matter. As the debate will likely become more active in the near future, the AMO will not be included in this research. In the time since the publication of Mann and others (2021) there has been an increasing body of AMO work, despite ongoing research, there is evidence for some acceptance of a paradigm shift in North Atlantic climatology based on this dynamic understanding.

#### **2.4 Ocean-Ice-Atmosphere Interactions on the Greenland Ice Sheet**

Recent mass loss on the Greenland Ice sheet has had a pronounced impact on iceberg generation through the impacts on tidewater glaciers. One of the main drivers of melt across the entirety of the Greenland ice sheet is ice-albedo feedback. Dark areas on the Greenland ice sheet due to surface meltwater or dark deposits lead to increases in net solar shortwave radiative flux and temperature, which exacerbate melt conditions in adjacent areas (van den Broeke et al., 2009; Box et al., 2012). These conditions lead to surface melt and glacier undercutting. Undercutting is the process that occurs at the Ice-Ocean interface at the terminus of a glacier where glacial surface meltwater will run to the base of the glacier through moulins and crevasses and continue to run toward the ocean. This cold, fresh water will continue to run under tidewater glaciers toward the ocean until reaching the terminus. Once the cold, fresh meltwater reaches the terminus of the glacier, and the saltier seawater that is present there, their densities will begin interacting. The fresh water begins to rise up the face of the glacier's until it reaches the sea surface. As this plume of cold fresh water

rises to the surface, warmer, saltier water replaces the cold water flowing out from under the glacier. This warmer saltier water that now resides under the glacier begins to melt the tidewater glacier from the bottom. This process is called undercutting. This undercutting weakens the structural integrity of the tidewater glacier, thinning it. (Rignot et al, 2015)

Additionally, recent Greenland mass loss has been attributed to increased surface runoff, changes in precipitation, and ice dynamics (Wood et al., 2018) such as basal sliding (Maier et al., 2019) where meltwater at the base of a glacier provides lubrication between the glacier and the bedrock beneath it, allowing it to move out to sea more rapidly.

In coastal environments, glacier responses to warming oceans vary. Glaciers with a floating tongue and therefore more area of interface with ocean waters are more subject to rapid retreat (Larsen et al., 2016). With coastal tidewater glaciers in Greenland being the source of North Atlantic icebergs, Rignot and others (2010) found that mass loss on tidewater glaciers attributed to submarine melt is twice that of surface melt and is directly related to iceberg discharge.

## **2.5 Iceberg Production and Transit**

Icebergs of the North Atlantic are primarily generated by the coastal outlet glaciers of Greenland's west coast. (Bigg, 2015). There are varied causes of iceberg generation, and influx into the open sea. Marsh and others (2018) determined that 1/3 of variation in the number of I48Ns can be attributed to ocean and atmospheric drivers, while 2/3 of the variation is related to discharge rates at the source. Models involved in quantifying this Greenland discharge have involved NAO-Index, Greenland SMB, and Labrador Sea SSTs as being important factors in iceberg production (Bigg et al, 2014, Zhao, et al. 2016). Marsh and

others (2018) additionally infer a 6–10-month lag time for an iceberg to transit from Greenland to the 48<sup>th</sup> Parallel. The IIP operates on a wider 1-3 transit period (IIP; 2016, IIP 2018; IIP, 2020).

Sea conditions are also a strong indicator of iceberg presence south of 48°N as these surface conditions are paramount to Iceberg survivability. FitzMaurice and others (2016) argue for the influence of sheared oceanic flow on the transit of I48Ns. The contributors conclude that icebergs move fastest when the entire draft (submerged portion of the iceberg) is entirely within the surface flow within their home fjord. FitzMaurice, Cenedese and Straneo (2017) later expand on this concept by concluding that the flow direction and magnitude around an iceberg. When flow is homogenous, meltwater plumes from the iceberg melt remain attached, and act as a protectant. However, when flow begins to flow around the iceberg draft, the upstream plume detaches, and follows the current around the rear of the iceberg increasing the rate of subsurface melt. Included within oceanic variables are variations in Labrador current (Bigg et al. 2014, Marsh et al., 2018).

In addition to source and oceanic forcings, atmospheric variables used previously in I48N modeling include wind (zonal and meridional), Temperature, humidity, long/shortwave radiation, and precipitation on timescales ranging from 3-hourly to daily (Dussin, et al. 2016, Marsh et al., 2018)

### 3. RESEARCH METHODS

#### 3.1 Study Site

This study is comprised of an array of a study sites, dependent on the variables being explored, and the analysis being conducted. The four major study areas are the Iceberg reconnaissance area, Labrador Sea ice observation area, NAO/AO Index Areas, and the case study area.

The primary study area is that of the International Ice Patrol dataset G10028 (IIP, 2020) which contains monthly counts of icebergs equal-to or greater-than 15m long at the water line sighted south of the 48<sup>th</sup> parallel north, just north of St. John's, Newfoundland. The spatial limits of dataset G10028 are between 48°N – 27°N, 36°W – 60°W (IIP Reconnaissance Area). The 48<sup>th</sup> Parallel as a threshold for this dataset originated with Edward Smith (1926) and has been used by the IIP thereafter. This line of demarcation was selected as most of the shipping lanes in the Western North Atlantic are found south of the 48<sup>th</sup> parallel, thus icebergs become much more threatening after crossing the 48<sup>th</sup> Parallel (Trivers, 1994; Rudnickas and Serumgard, 2018).

The sea ice data is collected from the Canadian Ice Service (CIS) Northern Labrador observation area, located between a northern boundary from 60.469 °N, 64.702 °W to 60.483 °N, 54.735 °W; and a southern boundary between 56.579 °N, 64.579 °W to 56.528 °N, 54.882 °W (Figure 3.1).

The North Atlantic Oscillation Index (NAOI) data is a discrete, quantitative variable to be used in the analysis of I48Ns, however this number is derived spatially, so discussion of the NAOI in the realm of study area is warranted. The NAOI products are available in two varieties, station-based and principal component (PCA) based. For this study, the PCA-based data is selected. The PCA-based NAOI is calculated through an Empirical Orthogonal

Function of SLPs across the North Atlantic (Hurrell et al, 2020b). The limitations for these datasets are outlined in section 3.3. The Arctic Oscillation index is derived similarly to the PCA-based NAOI, by projecting daily 1000hPa height anomalies north of 20°N onto a loading pattern of height anomalies averaged from 1979-2000.

The final study area is related to the case study area. The reanalysis data is projected onto an orthographic map projection centered on a point located at 48°N, 60°W. Using this projection, it is possible to examine transpolar data, as well as conditions in the North Atlantic, North America, Europe and North Africa. The qualitative analysis of these reanalysis data is largely focused on areas relevant to North Atlantic icebergs, specifically, Greenland, Baffin Bay, Davis Strait, Labrador Sea, Eastern Canada and the greater North Atlantic.

### **3.2 Methods and Data Analysis**

This study is divided into 6 phases. NAO/AO-Iceberg phase, Logistic Regression Phase, AIC model quality test, IRV testing phase, multiple regression phase, and case study phase.

#### **3.2.1 Iceberg Lag Times Through the Use of Linear Regression Modeling**

For the NAO/AO-Iceberg phase, basic linear regression models will be fit using PC-based NAOI, and AOI as Ide variables, and annual I48N data from dataset G10028 at 0-, 1-, 2- and 3-year time lags as response variables respectively. The formula for the linear regression is found in Equation 3.1. Where Y is the response variable (count of I48Ns),  $X_i$  is the predictor variable (NAOI/AOI),  $\beta_0$  is the y- intercept, and  $\beta_1$  is the slope.

$$Y_i = \beta_0 + \beta_1 X_i \quad (3.1)$$

The hypotheses for these linear regressions are  $H_0: \beta_1 = 0$ , there is no association between NAOI/AOI and number of I48Ns and  $H_a: \beta_1 \neq 0$ , there is an association between NAOI/AOI and the number of I48Ns.  $\beta_1$  is calculated using equation 3.2, where  $n$  is the number of years in the dataset (37),  $x$  is the predictor variable (NAOI/AOI), and  $y$  is the response variable (count of I48Ns).

$$\beta_1 = \frac{n(\sum xy) - (\sum x)(\sum y)}{n(\sum x^2) - (\sum x)^2} \quad (3.2)$$

After determining if there is an association between the predictor and response variables, further analysis can be completed to gain more information about the strength of the relationship, by calculating the correlation coefficient ( $r$ ) to determine the strength of the relationship; and coefficient of determination ( $R^2$ ) to determine the proportion of variance in the response variables explainable by the predictor variable. By identifying the combinations between predictor and response variables with the highest correlation coefficient ( $r$ ), it is possible to determine which time lag correlates most highly with each teleconnection index. This is valuable, as by finding the time lag period with the highest correlation coefficient, special attention can be given to that time period during subsequent phases of the research project. The full monthly counts of icebergs used in the analysis are found in Appendix I.

### 3.2.2 Logistic Regression Modeling Iceberg Count Based on NAO/AO

The logistic regression phase is designed to model the probability of the discrete outcome of iceberg severity at Light, Moderate, Heavy, and Extreme thresholds, with respect to NAOI and AOI. For the period of 1983 – 2020, iceberg year severity is broken into the following categories based on the count of I48Ns: Light (0-230), Moderate (231-1036), Heavy (1037-1398), and Extreme (1399-) (Rudnickas and Serumgard, 2018).

The logistic regression is selected, in this case, as the data meets the assumptions of the test, being, absence of perfect multicollinearity, absence of specification errors, independence of observations, and the use of binary dependent variables (Meyers, Gamst & Guarino, 2013). For this series of tests, each severity category is tested independently in a series of logistic regressions with a single binary predictor. Each iceberg year is categorized for the particular regression being performed. For instance, while testing Light iceberg years, any year with a count of icebergs between 0 and 230 will be categorized as 1, while all iceberg years outside of this range are categorized as 0. The full list of binary variables is available in Appendix II.

The logistic regression functions by producing a constant  $a$  and a regression coefficient  $b$ , which is calculated through maximum likelihood estimation of a logit (binary) variable (Meyers, Gamst & Guarino, 2013). The main output of a logistic regression is the probability of the occurrence of an event, in this case, if NAO/AO can predict the severity category of an iceberg year. The logistic regression calculates odds which can be further transformed into probability using the natural log ( $\ln$ ) of the odds. This relationship is described in equation 3.3, where  $\text{group}_{\text{pred}}$  represents predicted group membership,  $b$  coefficients represent change in log odds of membership in a group for a one-unit increase and  $x_1$  represents the predictor variable, in this case either NAOI or AOI. (Meyers, Gamst & Guarino, 2013).

$$\text{group}_{\text{pred}} = \ln[\text{odds}] = a + b_1 X_1 \quad (3.3)$$

After this analysis,  $\text{group}_{\text{pred}}$ , being the log odds, can be transformed into predicted probability for interpretation purposes. This is calculated by taking the antilog, as described in equation 3.4, where  $e$  is the exponent (Meyers, Gamst & Guarino, 2013).

$$\frac{e^{\text{group}_{\text{pred}}}}{1 + e^{\text{group}_{\text{pred}}}} = \text{predicted probability} \quad (3.4)$$

Finally, these results are plotted along a logarithmic curve, which present the response of changing probability of an iceberg year falling within a category with respect to the predictor, either NAOI or AOI, or a combination model. All models are run with a binomial distribution, with the exception of Extreme icebergs, which are run with a quasi-binomial distribution, due to the strong separability between the number of positive (1) and negative (0) binary variables.

### 3.2.3 AIC Testing of Model Fit

Akaike's information criterion (AIC) (Akaike 1973, Burnham and Anderson, 2002) is a statistical method that allows for the intercomparison of model fit based on the data it is comprised of. This method is able to determine the best model fit in a series of models, in this case, linear regression models. The AIC of a series of models can be used to determine which of the models explains the most variation in a model, with the fewest number of predictor variables.

For this test, a series of linear models are generated which feature a varying degree of influence of AO and NAO on Iceberg counts, these models being: NAOI Only, AOI Only, NAOI – AOI (Jones et. al 1997), NAOI + AOI, and NAOI x AOI. The purpose of this analysis is to determine whether the North Atlantic Oscillation or the Arctic Oscillation is the stronger driver of Iceberg Counts.

AIC is calculated using number of parameters (predictor variables) and maximum likelihood estimate, and is outlined in equation 3.5, Where k is the number of model

parameters (variables), and  $(\mathcal{L}(\hat{\theta}|y))$  is the numerical value of log-likelihood at its maximum point (Burnham and Anderson, 2002).

$$AIC = -2\log(\mathcal{L}(\hat{\theta}|y)) + 2k \quad (3.5)$$

A lower value for AIC indicates a better model fit, and therefore a stronger relationship. It is worth noting that the design for this test is meant to ensure that a well-founded group of models is selected to answer the specific questions, as the strongest AIC in a given set may be only the strongest among a weak set of models if consideration is not taken (Burnham and Anderson, 2002).

#### 3.2.4 NAO/AO as a Driver of Sea Ice Maximum Extent

Testing of NAO/AO as drivers of Maximum Sea Ice Extent takes the form of an additional Linear Regression phase. This phase uses data derived from the Canadian Ice Service (CIS) IceGraph for the area of Northern Labrador, coupled with existing NAO and AO index values used in previous stages. This portion's statistics are tested at 0-, 1-, 2-, and 3-year lags. As this segment examines a different climatic outcome than previous stages, all lag periods are tested, and will not be informed by the lag determined to be the best fit by the analysis described in section 3.2.1. These regressions utilize the same process described by equations 3.1 and 3.2, using NAO/AO Index respectively as the predictor variables, with maximum ice coverage as a percentage of observation area as the response variable. This sea ice data is observed in the Canadian Ice Service's Northern Labrador Ice Reconnaissance Region, in an observation area spanning between a northern boundary from 60.469 °N, 64.702 °W to 60.483 °N, 54.735 °W; and a southern boundary between 56.579 °N, 64.579 °W to 56.528 °N, 54.882 °W. This portion is designed to examine the correlation between NAO/AO and the development of Sea Ice along the Labrador coast.

### 3.2.5 Sea Ice Maximum as a Driver of I48Ns

Sea Ice along the Labrador coast bears a strong connection to the number of I48Ns detected in a year. Coastal Sea Ice in the Labrador Sea acts as a buffer to icebergs keeping them in the oceanic current. When there is little sea ice in the region, icebergs are more likely to become stranded on beaches, never continuing their transit to ultimately cross the 48<sup>th</sup> Parallel. (IIP, 2016; IIP, 2018)

This relationship is examined in this research segment. Continuing with the same linear regression method described by equations 3.1 and 3.2, this time with Sea Ice Maximum Percentage as the predictor variable, and the number of I48Ns as the response. This series of tests is designed to examine the relationship between Sea Ice Maximum and I48Ns at 0-, 1-, 2-, and 3-year lags.

### 3.2.6 Case Studies

Six cases studies, comprising the most recent three years with the highest number of I48Ns and the three most recent years with the lowest number of I48Ns. These case studies include the high (I48N) ice years 2014(1546), 2019(1515), 2009(1204) and low I48N ice years 2010 (1), 2011(3), and 2013 (13). These case studies use a combination of NCEP/DOE Reanalysis II reanalysis models (Kanamitsu et al., 2002) to examine the spatial meteorological and climatic conditions in the iceberg transit path in the year prior to the ice year being examined. As sea ice, SST/skin temperature, zonal wind and meridional wind are not available variables on the NCEP/DOE Reanalysis II, these variables are derived from NCEP/NCAR Reanalysis I (Kalnay et al., 1996, Kistler et al., 2001). In order to examine variation changes more closely, reanalysis output is generated to represent anomalies, or difference from climatological normal (1981-2010) rather than mean of the data. This method allows for above and below normal conditions to be analyzed more easily.

This method facilitates greater understanding of the physical meteorology and oceanography involved in I48N presence in a given year and allows for a complete picture of the events that can lead to I48N presence. The reanalysis products that will be incorporated into the case studies are outlined in Table 1.1.

## 4. RESULTS

### 4.1 Iceberg Lag Times Through Use of Linear Regression Modeling

Testing of lag times through the use of linear regression modeling produced consistent results between both NAOI and AOI as predictor variables with I48N counts as the response variable respectively (Figure 4.1). When examining the relationship between NAOI and I48Ns at 0-, 1-, 2- and 3-year lags (Table 4.1), only the 1-year lag is significantly correlated ( $p = 0.00646$ ). With a correlation coefficient of  $r = 0.43$ , this relationship is moderately correlated. However, given the coefficient of determination of  $R^2 = 0.1885$ , NAO is responsible for a portion of less than 19% of variability in I48Ns at this temporal resolution, this, when compared to the other lags tested, is a dramatic strengthening. The significance of this result is further verified by the strong t-value of 2.892, being nearly 3 standard deviations from zero, and 1.3 more than the next nearest temporal lag period.

The case is similar when examining AOI as the predictor variables (Table 4.2). Like with the NAO, the 1-year lag is the only temporal lag period where there is a significant correlation ( $p = 0.0349$ ) between AOI and I48Ns, albeit it weaker than the correlation between NAOI and I48Ns. This significant correlation at the 1-year lag has a correlation coefficient of  $r = 0.34$  considered weakly-to-moderately correlated. With a coefficient of determination of  $R^2 = 0.118$ , only about 12% of the variance in I48N counts can be attributed to changes in AOI, compared to 19% of NAOI. With a t-value of 2.192, the influence of AOI at a 1-year lag is much closer to the other examined AOI lag periods than was the case with NAO. The result of this test informs the temporal lag period to be examined in subsequent tests, being 1-year.

## 4.2 Logistic Regression Modeling Iceberg Count Based on NAO/AO

Of the 12 Logistic regressions performed (Figure 4.2), there are two statistically significant results. Both of these significant results are a result of models where NAO is either the sole predictor variable or is a predictor variable in a multivariate logistic regression model, when Extreme I48Ns are the response variable, at a 1-year lag. Beginning with NAO as the predictor variable and Extreme I48Ns as the response, a parameter estimate of 4.3674 suggests that the likelihood of an extreme iceberg year is increased during years with a high NAOI value. Along with being statistically significant ( $p = 0.009616$ ; 95% CI = 1.551, 8.418) this model also has the highest z-value, indicating greater certainty than other models tested.

Interestingly, when both NAO and AO are incorporated into a multivariate model where Extreme icebergs are the response variable, only the influence of the NAO is significant ( $p = 0.01513$ ; 95% CI=1.507, 9.722). This model has a stronger estimate (4.8562) than both NAO on its own, and AO in the same multivariate model, showing the strong likelihood of an extreme iceberg event in years with a higher NAOI value. The z-value is also strong ( $z = 2.429$ ), second only to NAO on it own, which shows lower uncertainty than other models. Both NAO alone and NAO within the NAO/AO multivariate model have the lowest AICs of all other models, showing the strength of model fit when examining extreme iceberg years.

## 4.3 Model Fit based on Akaike's Information Criterion

The AIC testing phase is designed, given the pattern of stronger NAO influence in previous tests in comparison to AO, to examine the strength of various linear regression models, each with increasing influence of AO on the number of I48Ns at a 1-year lag. The five models when organized by AIC, where lower AIC is representative of better model fit, is ordered in a pattern that suggests that the more influence of AO is present in a regression

model, the weaker the fit is of the model (Table 4.4). Delta AIC represents the difference between each model and the model with the best fit. In this case, both NAO only and NAO – AO models are equally well fit. However, models with the most influence of AO as variable, namely NAO x AO and AO Only have a Delta AIC of 4.29 and 4.23 respectively, more than double that of the NAO + AO model with a delta AIC of 2.14. Both the NAO and NAO – AO models have the same AIC Weight (AIC Wt.), where 39% of total variation in the I48N dataset can be described by NAO. This is striking when compared to the AO only model, which has an AIC Wt. of 0.04, suggesting that only 4% of variation in I48Ns is attributable to AO only.

#### **4.4 NAO/AO as a Driver of Sea Ice Extent**

Testing NAO/AO correlation with sea ice maximum on the Northern Labrador coast at 0-, 1-, 2-, and 3-year lags yielded results inconsistent with previous analyses, in which NAO has been shown to be a stronger influence on iceberg presence. In this analysis, NAOI did not result in any statistically significant correlations at any of the tested lags. The strongest of these non-significant results was at one year, with a correlation coefficient of  $r=0.27$ , and a p-value of 0.094 (Table 4.5). The Arctic Oscillation Index was a stronger predictor variable in this case, yielding a significant result at a one-year lag, similar to previous analyses. At a one-year lag, AO yielded a correlation coefficient of  $r = 0.389$ , and a coefficient of determination of 0.1515, stating that 15% of variability in Sea Ice Maximum can be attributed to AO at a one-year lag. This relationship carries a p-value of 0.0157 (Table 4.6).

#### **4.5 Sea Ice Maximum as a Driver of I48Ns**

With a suggested connection between sea ice on the Labrador coast, and the number of I48Ns surviving to cross the 48<sup>th</sup> parallel (IIP, 2016; Rudnickas and Serumgard, 2018),

testing the correlation between the maximum sea ice coverage as a percentage of observation area and I48Ns at 0-, 1-, 2-, and 3-year lags is an opportunity to further explain previously explored connections. Both the 0- and 1-year lags in this analysis were statistically significant (Table 4.7). The 0-year lag has a correlation coefficient ( $r$ ) of 0.5664, a moderately strong correlation. This lag also has a strong coefficient of determination ( $R^2$ ) of 0.3208, indicating that the presence of Sea Ice in Northern Labrador is responsible for 32% of variation in the number of I48Ns detected in the same year. This relationship is strongly statistically significant, with a p-value of 0.00021.

The relationship between sea ice maximum percentage and I48Ns at a 1-year lag was also strongly significant ( $p=0.00071$ ), albeit slightly weaker than the 0-year lag. This relationship has a correlation coefficient of 0.5252, a strong correlation. The coefficient of determination of 0.2758 indicates that 27% of variation in the number of I48Ns detected in the following year.

## 4.6 Case Studies

### 4.6.1 Geopotential Height (500 hPa)

Geopotential height (GPH) is the height above sea level where a particular pressure level is measured, in this case 500hPa. 500hPa is on average observed at an altitude of 5.5km (Barry and Hall-McKim, 2014). This height is a result of two meteorological phenomena, the negative exponential nature of pressure changes with altitude, and the counterforce of downward gravitational acceleration which is represented by the hydrostatic equation (Equation 4.1) where  $\delta p$  is change in pressure,  $\delta z$  is change in height,  $g$  is the acceleration gravity and  $\rho$  is atmospheric density. (Barry and Hall-McKim, 2014)

$$\frac{\delta p}{\delta z} = -g\rho \quad (4.1)$$

High geopotential heights indicate the presence of calm weather do to sinking air associated with high pressure. Inversely, low geopotential heights indicated rising air associated with low pressure, indicating the potential for convective weather. (Barry and Hall-McKim, 2014)

Examining the mean conditions during the lowest iceberg years (2010, 2011, and 2013), the defining feature is found in the area directly above the West Greenland iceberg source glaciers. The 500hPa geopotential height anomaly here is between 40 and 50 meters above the climatological mean, indicating calmer than normal conditions. Weaker positive GPH anomalies radiate outward from this central value, encompassing all of maritime Canada in values between 10 and 40 meters above the mean. (Figure 4.6.1)

During the high iceberg years (2014, 2019, and 2009), there is a stronger negative anomaly present of -25 meters over North-Central North America, extending into the central Hudson Bay. The gradient in anomaly value begins to shift toward the positive near Baffin Island, with much lower, yet still above average anomalies in the iceberg source region in West Greenland. (Figure 4.6.1)

#### 4.6.2 Relative Humidity

When reanalysis of relative humidity (RH) during high and low iceberg years are examined, there is negligible difference between the two, indicating that RH is not driving icebergs as strongly as other phenomena examined by reanalysis (Figure 4.6.2)

#### 4.6.3 Omega

Omega is a method of estimating vertical motion in the atmosphere. This is derived by the Omega Equation (Holton, 1992), which is composed of two terms, Differential vorticity advection, and thickness advection. (NWS, 2009). These terms can be described

essential as the amount of large-scale rotation, and the warm air present in the atmosphere in the area being studied. High Omega values are indicative of rising air, and convective weather, including precipitation. (NWS, 2009)

During the low iceberg years, Nearly the entire study area is within the climatological mean, with a notable exception above Scoresby Sound in East Greenland, where omega values are 0.06 Pa/s higher than the climatological mean. With that exception, the bulk of the area relevant to iceberg production and transit are under normal climatological conditions.

During the High iceberg years, most of mainland Greenland and the entire west coast of Greenland are experiencing omega higher than the climatological mean between 0.01 and 0.03 Pa/s. A small exception is present in a small oceanic region east of Cape Farewell, which is experiencing slightly lower (0.02 Pa/s) than climatological mean omega.

#### 4.6.4 Sea Ice

Sea ice (Figure 4.6.4) is revisited in this case study, with a greater geographic area. With the statistical portion found in section 3.2.5 focusing on the coastal area of Northern Labrador, reanalysis allows qualitative analysis of conditions in the entire iceberg transit path.

In ice years with the lowest number of icebergs (Figure 4.6.4), there is a negative sea ice anomaly along the entire Eastern Canadian coastline, and across Davis Strait. This anomaly indicates a below average amount of sea ice in the area, which is in line with the strong correlation between sea ice and I48Ns at the 0-year lag described in section 3.2.5. This reanalysis contributes some specificity to this simple correlation, by denoting the lack of icebergs when coastal sea ice is low.

Alternatively, in the high iceberg years, all oceanic areas relevant to the transit of icebergs from west coast of Greenland to the North Atlantic are nearer to the climatological mean.

#### 4.6.5 Sea Level Pressure

Sea Level pressure (Figure 4.6.5) is a good indicator of mean meteorological conditions, as low pressure is associated with convective weather, and high pressures are associated with clear conditions. During the low iceberg years, sea level pressures over Greenland, Baffin Bay and Labrador Sea are between 1-4 millibars above average, while during the high iceberg years, conditions in southwest Greenland, and Labrador Sea are slightly lower than the climatological mean. With such small differences in pressure from the climatological mean, it is unlikely that that is a dramatic impact on the number of I48Ns observed. However, Sea Level Pressure and Geopotential height in this instance both show higher than normal pressures between Sea level and 500hPa during low iceberg years. Given the relationship between the NAO and AO and atmospheric pressures in this region, this analysis warrants further study.

#### 4.6.6 Skin Temperature/ Sea Surface Temperature

According to the Group for High Resolution Sea Surface Temperature (GHRSSST), Near sea surface temperatures are subject to three physical processes: insolation absorption in the first few meters of ocean depth, heat loss to the atmosphere, and subsurface turbulent mixing. (Katsaros et al. 1977, GHRSSST, 2012). All of these factors contribute to the amount of heat stored in the area on the ocean-side of the ice-ocean interface, and that is able to be exchanged with the atmosphere. Due to the nature of this relationship, diurnal cycles and wind speeds can both have similar influence on Ocean-Atmosphere interface heat exchange. There are varied estimates for the thickness of the skin layer where this interface energy

exchange occurs, with some estimates of a few millimeters (Katsaros et al. 1977), to less than a millimeter (Hanafin, 2002). The importance of this skin layer ( $SST_{skin}$ ) in the energy exchange at the ocean-air boundary on icebergs is revealed in this analysis.

During low Iceberg years (Figure 4.6.6),  $SST_{skin}$  Temperatures in Baffin Bay, and Labrador Sea are all above the climatological mean, with temperate along the west coast of Greenland between 4-5 K above climatological mean. These warmer than normal conditions on the sea surface along the Labrador coast, is expected, given the below average concentration of Sea Ice observed during these same low iceberg years.

During the high iceberg years, there is again some above normal  $SST_{skin}$  conditions in Baffin Bay, where Icebergs originate. However, the  $SST_{skin}$  along the Labrador coast is within climate normal parameters. This, and the sea ice study, suggests that normal  $SST_{skin}$  conditions along Labrador coast would allow for coastal sea ice to form, which will enable icebergs to transit into the North Atlantic and eventually south of the 48<sup>th</sup> Parallel.

#### 4.6.7 Air Temperature

Air temperature (Figure 4.6.7) is a crucial aspect of the energy budget of ice, especially calved icebergs. While much of the iceberg remains submerged underwater. The ocean-air interface described in section 4.6.6, becomes more complicated when observed in the presence of an iceberg. This new Ocean-Ice-Atmosphere interface is going to determine the melting of the icebergs. Furthermore, as discussed in section 4.6.6 and mentioned in 4.6.4, in areas like Labrador Sea that form new sea ice annually, the annual air temperature has a strong influence on if that ice forms, and to what size and thickness. The exchange of energy between Air and Ice, Ice and Ocean, and Air and Ocean creates a complicated physical situation. Warm, often wet air present in an Ice-Atmosphere interaction will lead to

melting/sublimation of exposed ice, resulting in mass loss. One gram of airborne water vapor condensing on an iceberg releases enough heat to melt 8 grams of ice (Patterson, 1994). At the same time, the Atmosphere-Ocean interface, covered in section 4.6.6 is a factor in sea surface temperatures. The Ice-Ocean interface is also interesting, as water from melting icebergs remains on the surface for a time, due to the fresh water's lower density.

In the low iceberg years, all of Greenland, Baffin Bay and Labrador Sea are experiencing higher than normal surface air temperatures. This observation again lends itself to the influence of sea ice in this region, as these years with warmer-than-normal temperatures also have decreased sea ice.

In the high iceberg years, the area around West Greenland, Baffin Bay and parts of Labrador Sea are all again experiencing higher than normal temperatures, but to a lesser extent than in the low iceberg years. An interesting difference in these two periods emerges in Southern Labrador and Newfoundland, which is still within the climate normal. The largest portion of coastal Labrador Sea is between 0.4 and 1.2 Kelvins greater than normal, while in the low iceberg years temperatures on the Labrador coast are between 1.2 and 2.8 Kelvins higher than normal, a strong difference in expected similarly warm temperatures.

#### 4.6.8 Zonal Wind

Zonal Winds, or winds that travel along latitudinal lines, are important to the development of sea ice in Labrador Sea. Zonal winds, in the case of the Labrador coast involves Westerly winds. Westerly winds in a coastal environment, blowing from land to ocean pushes developing sea ice away from the coast, leading to thinner sea ice, and more area of open water (Fenty and Heimbach, 2013). However, in the area of the Labrador Shelf, during one spring study, ice moved at 2.5% of the wind magnitude. (Greenan and

Prinsenber, 1998). Greenan and Prinsenber (1998) also found that 57% of variance in the top 3m of ocean on the Labrador Shelf is attributable to winds. In this case, negative zonal wind represents easterly winds, while positive represents negative winds.

During the low iceberg years (Figure 4.6.8), zonal winds along the Labrador shelf were more easterly than normal, compared to 0.4m/s westerlies during high iceberg years. While this pattern on the surface seems counterintuitive to the explanation found in Fenty and Heimbach (2013), the <1m/s difference in zonal wind direction, coupled with the small impact of actual ice movement, and remaining 43% of unattributed influence in ice movement described by Greenan and Prinsenber (1998), potentially reveals other stronger influences in the development of coastal sea ice on the Labrador shelf than zonal wind magnitude.

During high iceberg years, A large pocket of westerly winds sits to the north of a large pocket on easterly winds in the North Atlantic. The presence of an extended area of wind shear is an interesting observation which also requires further study.

#### 4.6.9 Meridional Wind

Meridional Wind, as opposed to zonal wind, moves in a poleward direction. Meridional wind at the boundary of the Arctic and the mid latitudes is often a strong source of warm/cold air advection. Meridional flows at these latitudes carry warm air from the mid latitudes to the pole, and cold air from the pole to the midlatitudes (Francis and Vavrus, 2012; 2015). At this latitude, where the Arctic and midlatitudes interface, an increase in meridional flow is often coupled with a decrease in zonal flow at the synoptic and greater scales.

During the low iceberg years, (Figure 4.6.9) there is little variation from climatic normal in West Greenland, Baffin Bay and Labrador Sea, the exception to this normal in the relevant geographic regions is a slight pattern of northerly winds of  $\sim -0.4$  m/s in southern Labrador and Newfoundland.

During high Iceberg years, there is a northerly wind anomaly present on both sides of Greenland, with anomaly values ranging from 1 m/s to -0.25 m/s difference than climatological normal. There is a similarly weak southerly anomaly in central Greenland, around 0.25 m/s above climatological normal.

## 4.7 Chapter 4 Figures

Figure 4.1(a) AO/NAO v. I48Ns (0-Year Lag)

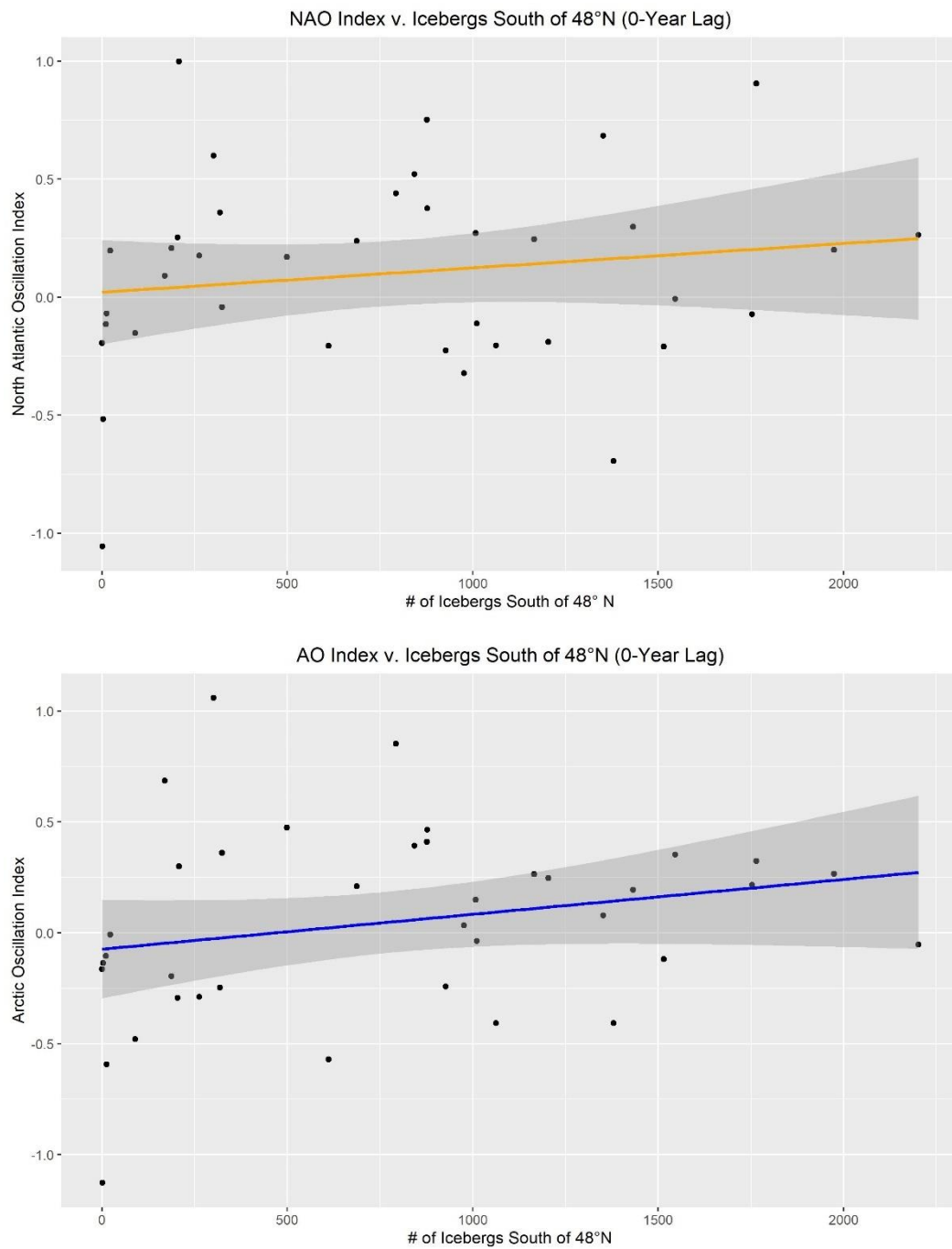


Figure 4.1(a) 0-Year Linear Regression plot of NAO (Top), AO (Bottom) and Number of Icebergs detected South of 48°N. Grey area denotes 95% CI.

NAO:  $r = 0.1559$ ,  $p=0.3499$ ,

AO:  $r = 0.20$ ,  $p=0.1601$

Figure 4.1(b) AO/NAO v. I48Ns (1-Year Lag)

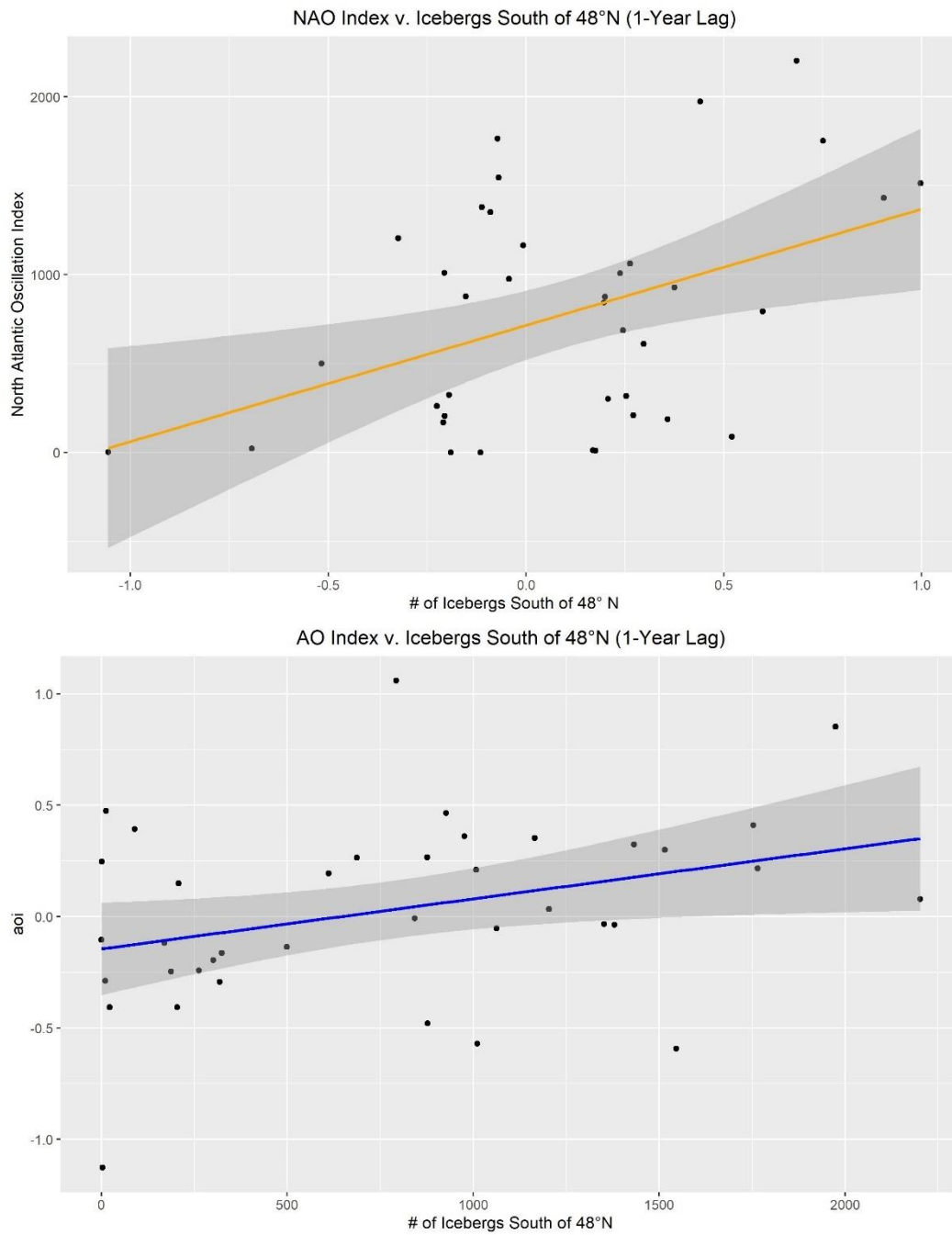


Figure 4.1(b) 1-Year Linear Regression plot of NAO (Top), AO (Bottom) and Number of Icebergs detected South of 48°N. Grey area denotes 95% CI. Bold denotes significance.

**NAO:  $r = 0.4341$ ,  $p=0.00646$ ,**

**AO:  $r = 0.3432$ ,  $p=0.0349$**

Figure 4.1(c) AO/NAO v. I48Ns (2-Year Lag)

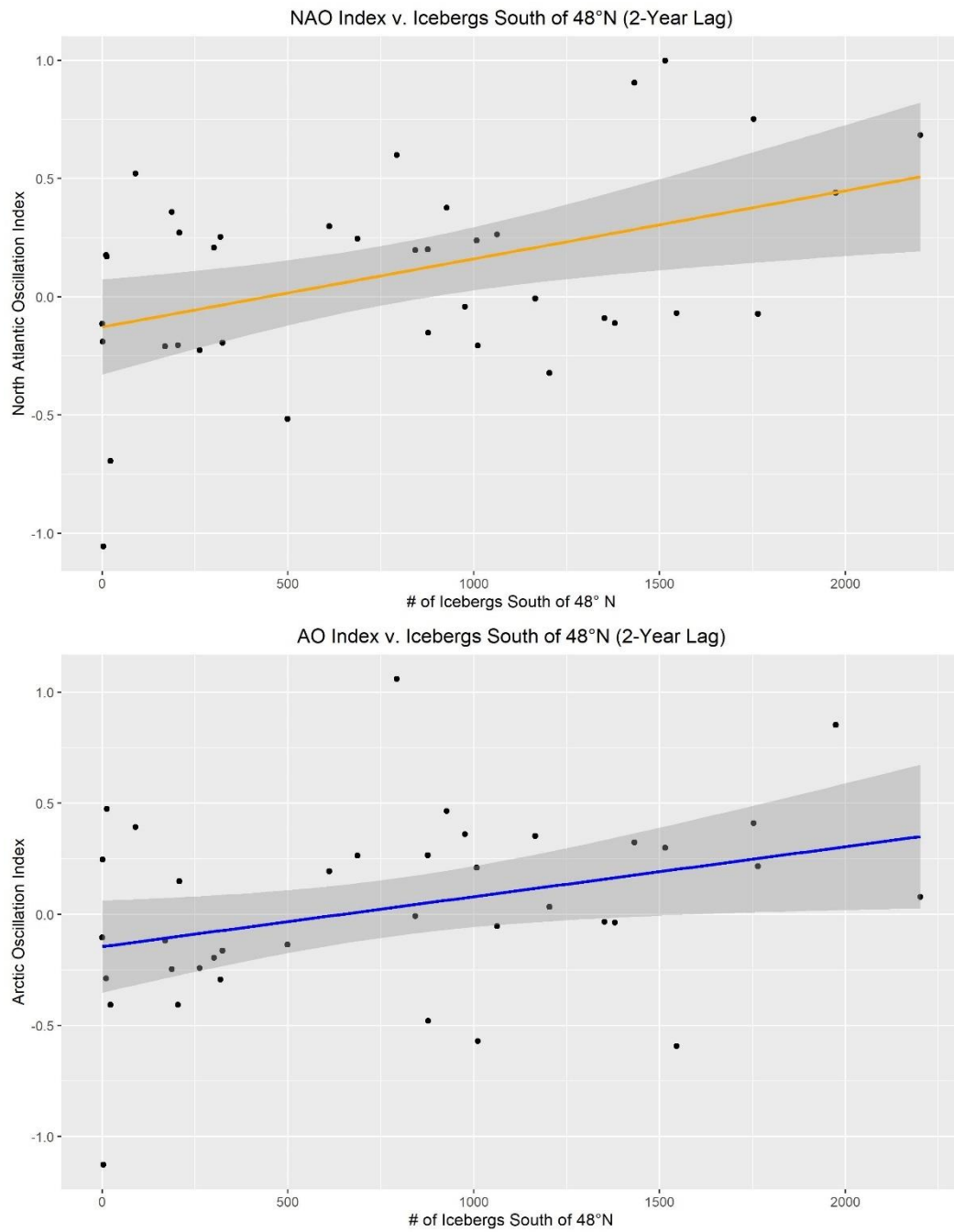


Figure 4.1(c) 2-Year Linear Regression plot of NAO (Top), AO (Bottom) and Number of Icebergs detected South of 48°N. Grey area denotes 95% CI.

NAO:  $r = 0.1636$ ,  $p=0.3301$ ,

AO:  $r = 0.2622$ ,  $p=0.116$

Figure 4.1(d) AO/NAO v. I48Ns (3-Year Lag)

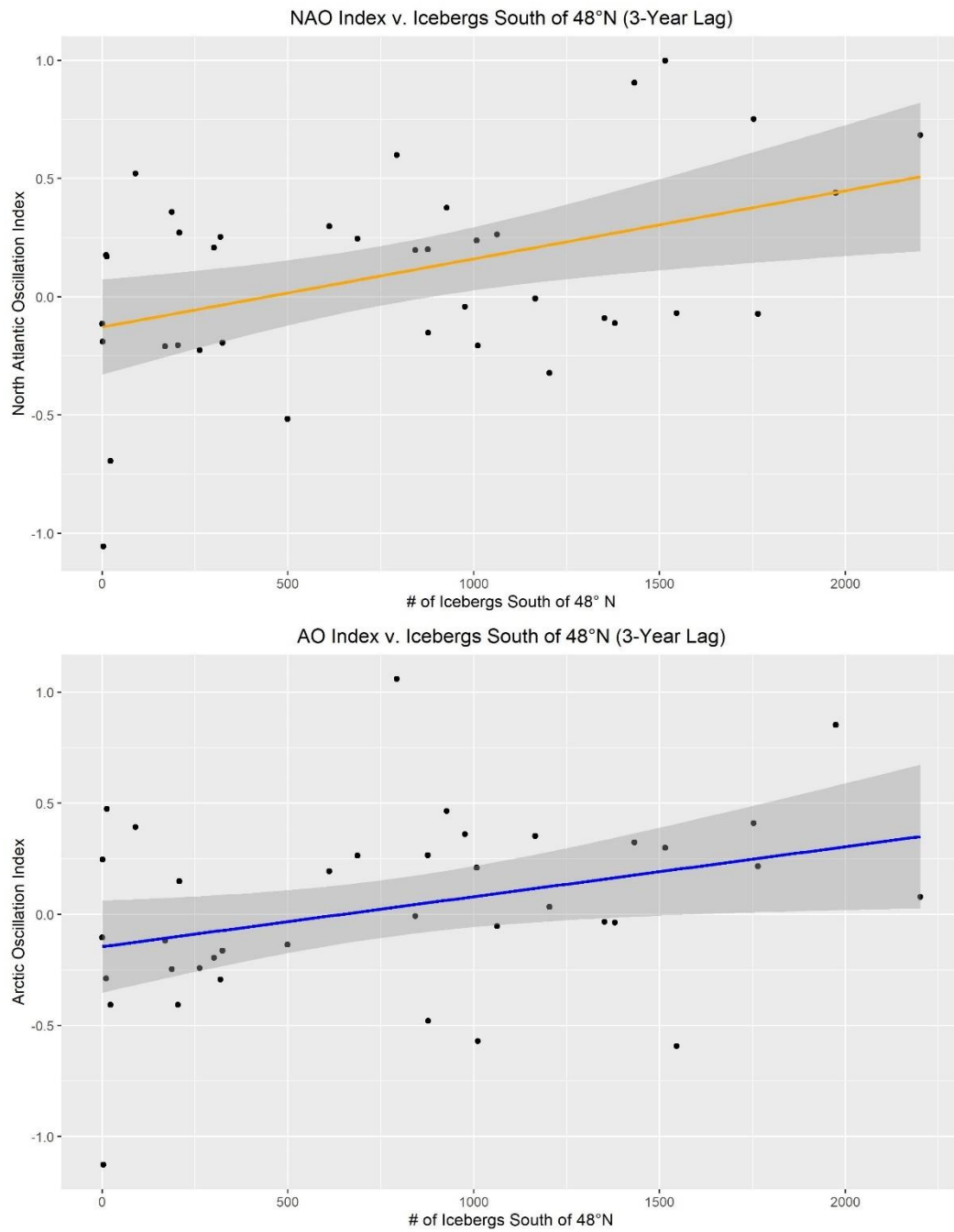


Figure 4.1(d) 3-Year Linear Regression plot of NAO (Top), AO (Bottom) and Number of Icebergs detected South of 48°N. Grey area denotes 95% CI.

NAO:  $r = 0.2446$ ,  $p=0.1388$ ,

AO:  $r = 0.2488$ ,  $p=0.132$

Figure 4.2(a) Logistic Regression, North Atlantic Oscillation

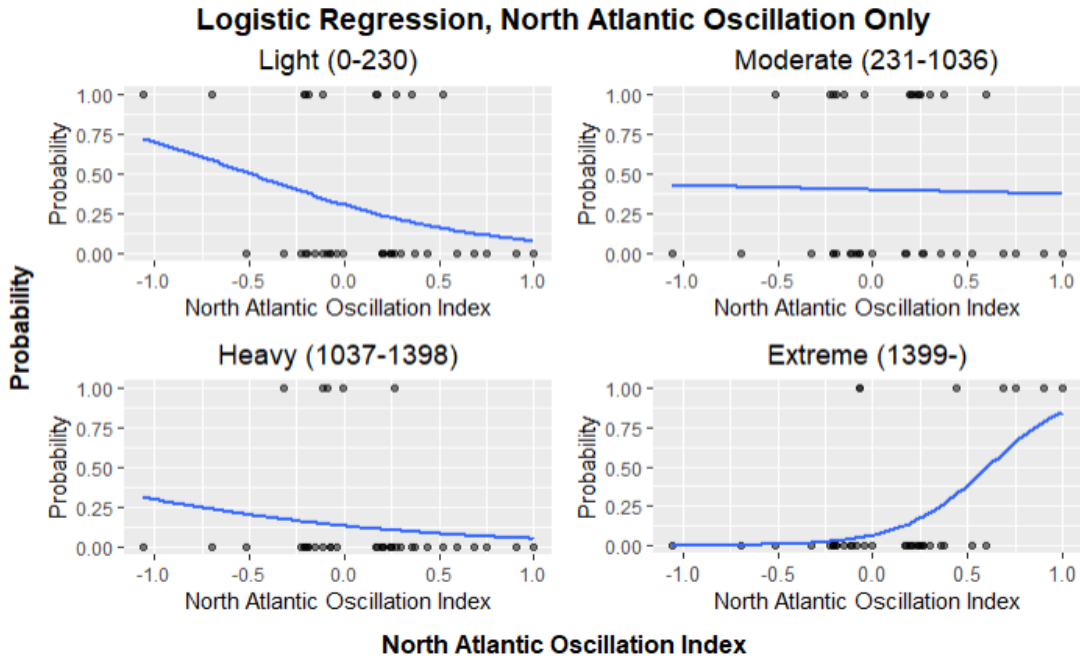


Figure 4.2(a) Logistic Regressions of North Atlantic Oscillation as a driver of I48N year categories Light, Moderate, Heavy, and Extreme and a 1-year lag. In this case, Extreme Icebergs are statistically significant.

Figure 4.2(b) Logistic Regression, Arctic Oscillation

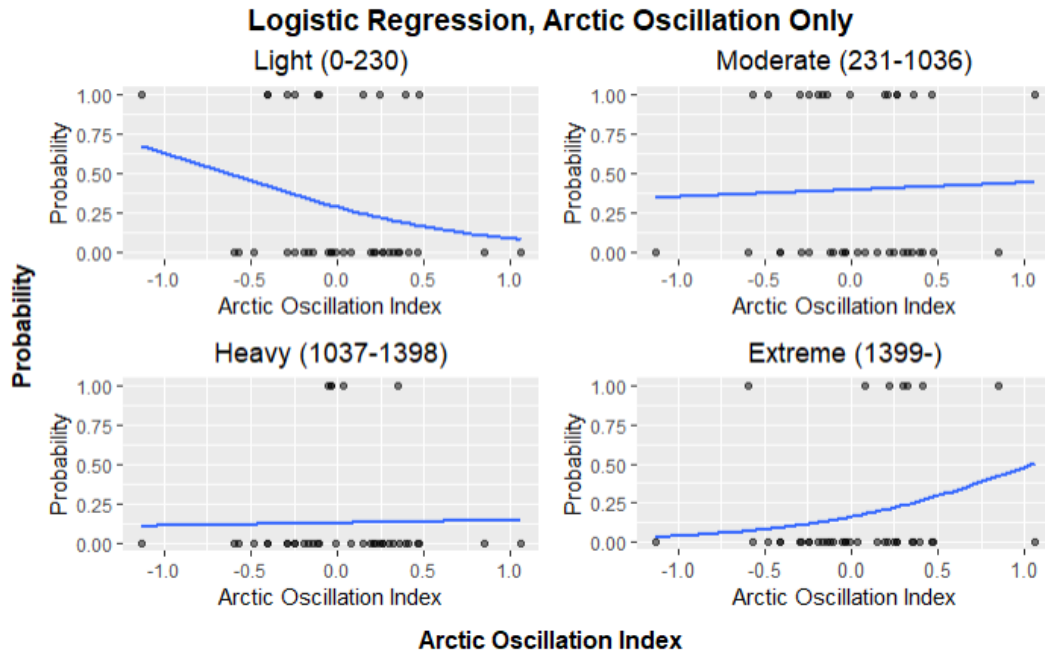


Figure 4.2(b) Logistic Regressions of Arctic Oscillation as a driver of I48N year categories Light, Moderate, Heavy, and Extreme and a 1-year lag. In this case, no models are statistically significant.

Figure 4.2(c) Logistic Regression, AO and NAO

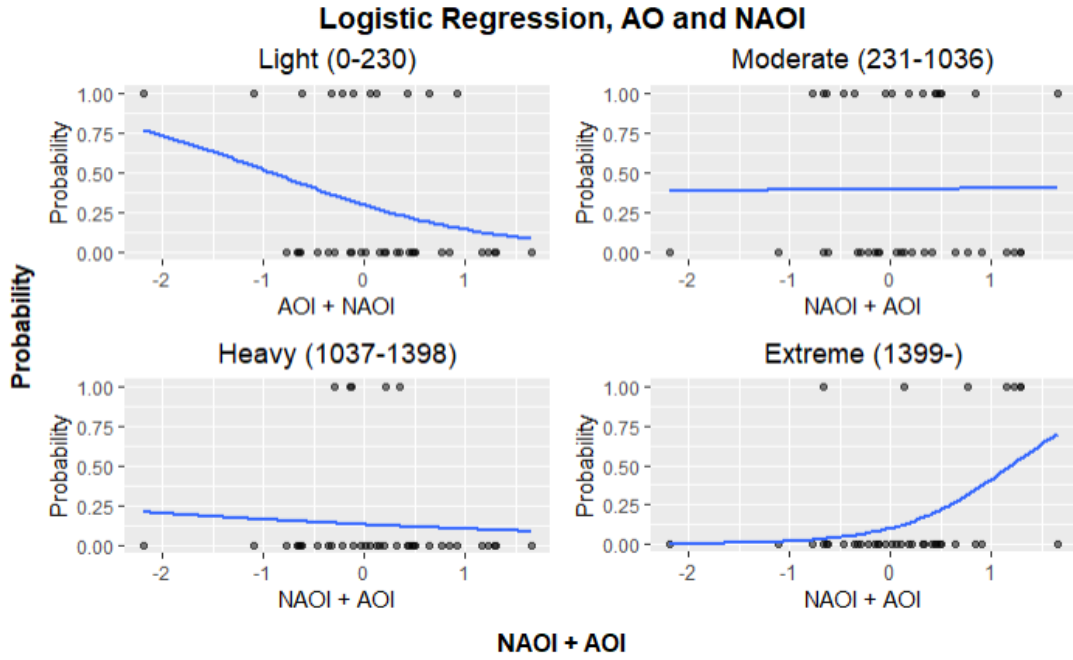


Figure 4.2(c) Logistic Regressions of North Atlantic Oscillation as a driver of I48N year categories Light, Moderate, Heavy, and Extreme and a 1-year lag. In this case, Extreme Icebergs are statistically significant.

Figure 4.3(a) AO/NAO v Maximum Sea Ice Concentration (0-Year Lag)

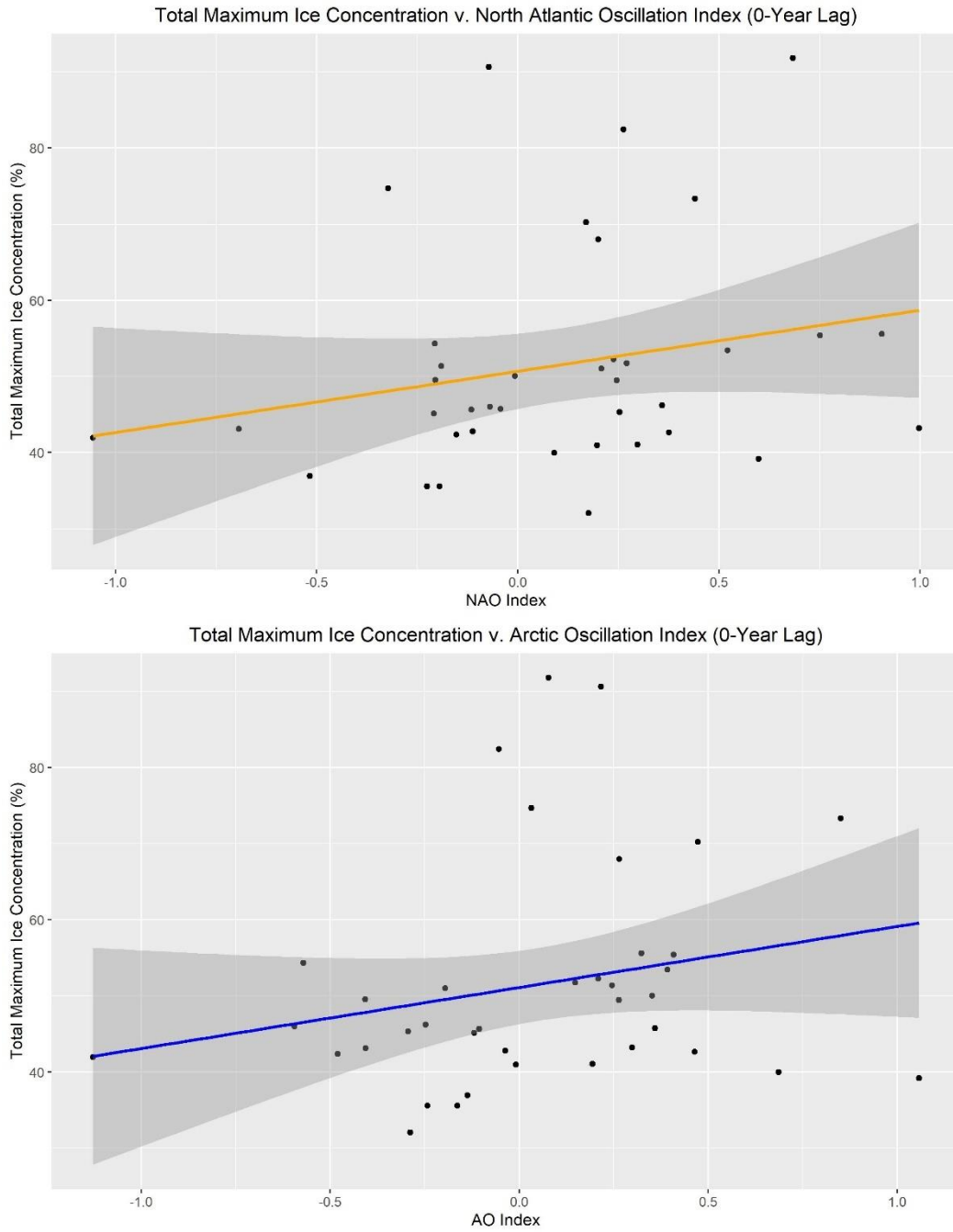


Figure 4.3(a) 0-Year Linear Regression plot of NAO (Top), AO (Bottom) and Total Maximum Sea Ice Coverage in Northern Labrador. Grey Area denotes 95% CI.

NAO:  $r = 0.2266$ ,  $p=0.171$ ,

AO:  $r = 0.2310$ ,  $p=0.163$

Figure 4.3(b) AO/NAO v Maximum Sea Ice Concentration (1-Year Lag)

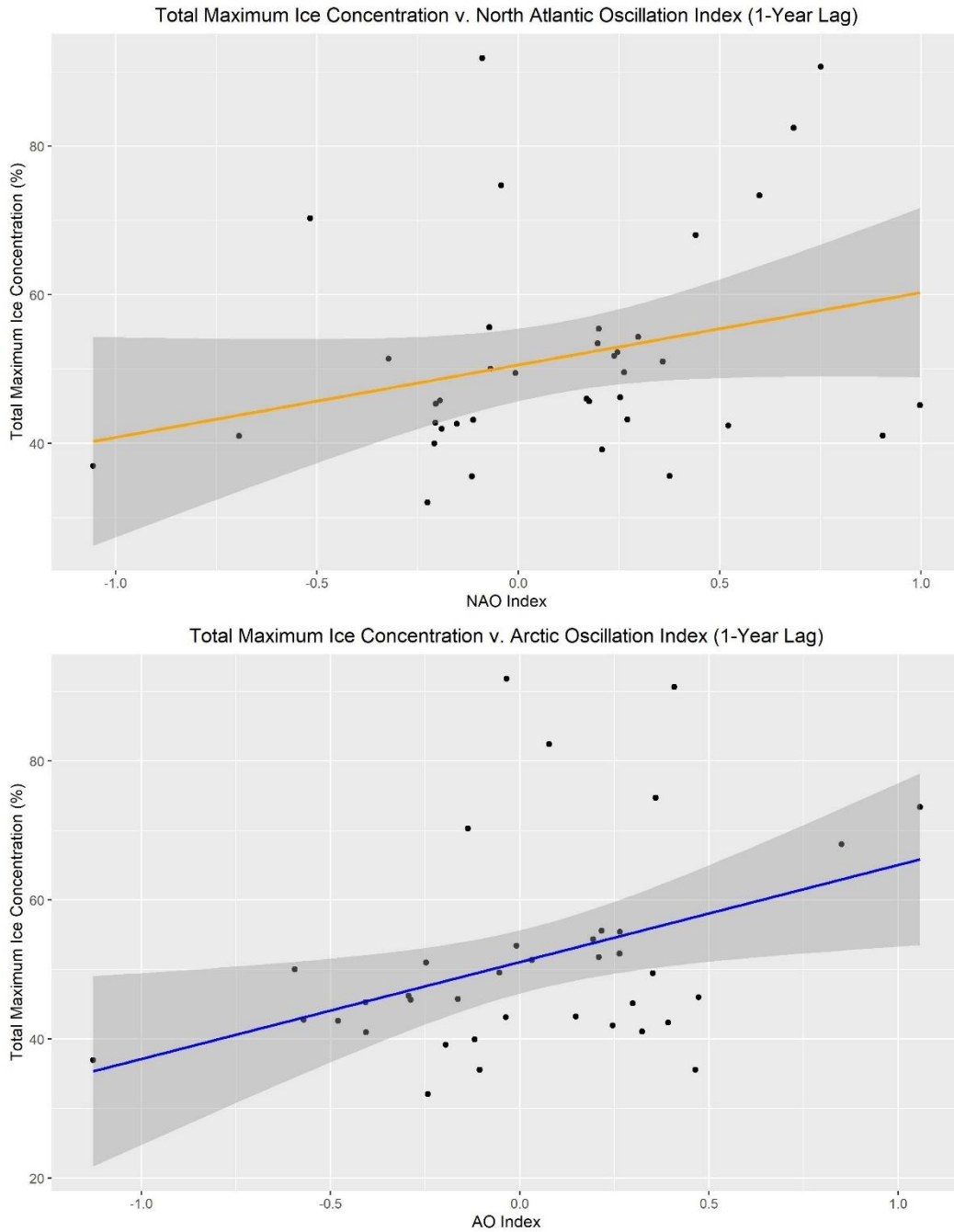


Figure 4.3(b) 1-Year Linear Regression plot of NAO (Top), AO (Bottom) and Total Maximum Sea Ice Coverage in Northern Labrador. Grey Area denotes 95% CI. Bold denotes significance.

NAO:  $r = 0.2755$ ,  $p=0.094$ ,

**AO:  $r = 0.3891$ ,  $p=0.0157$**

Figure 4.3(c) AO/NAO v Maximum Sea Ice Concentration (2-Year Lag)

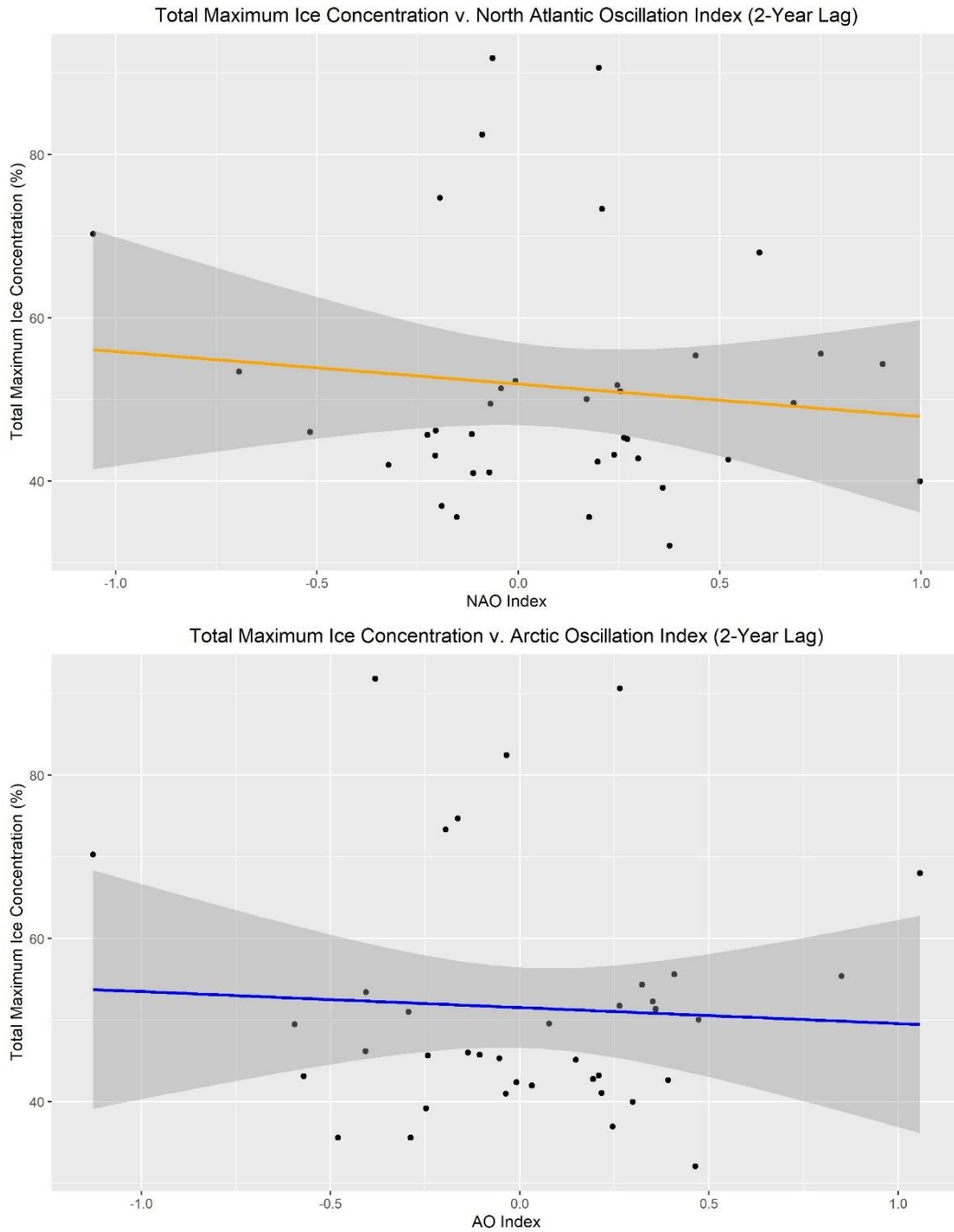


Figure 4.3(c) 2-Year Linear Regression plot of NAO (Top), AO (Bottom) and Total Maximum Sea Ice Coverage in Northern Labrador. Grey Area denotes 95% CI.

NAO:  $r = -0.111$ ,  $p=0.503$ ,

AO:  $r = -0.055$ ,  $p=0.742$

Figure 4.3(d) AO/NAO v Maximum Sea Ice Concentration (3-Year Lag)

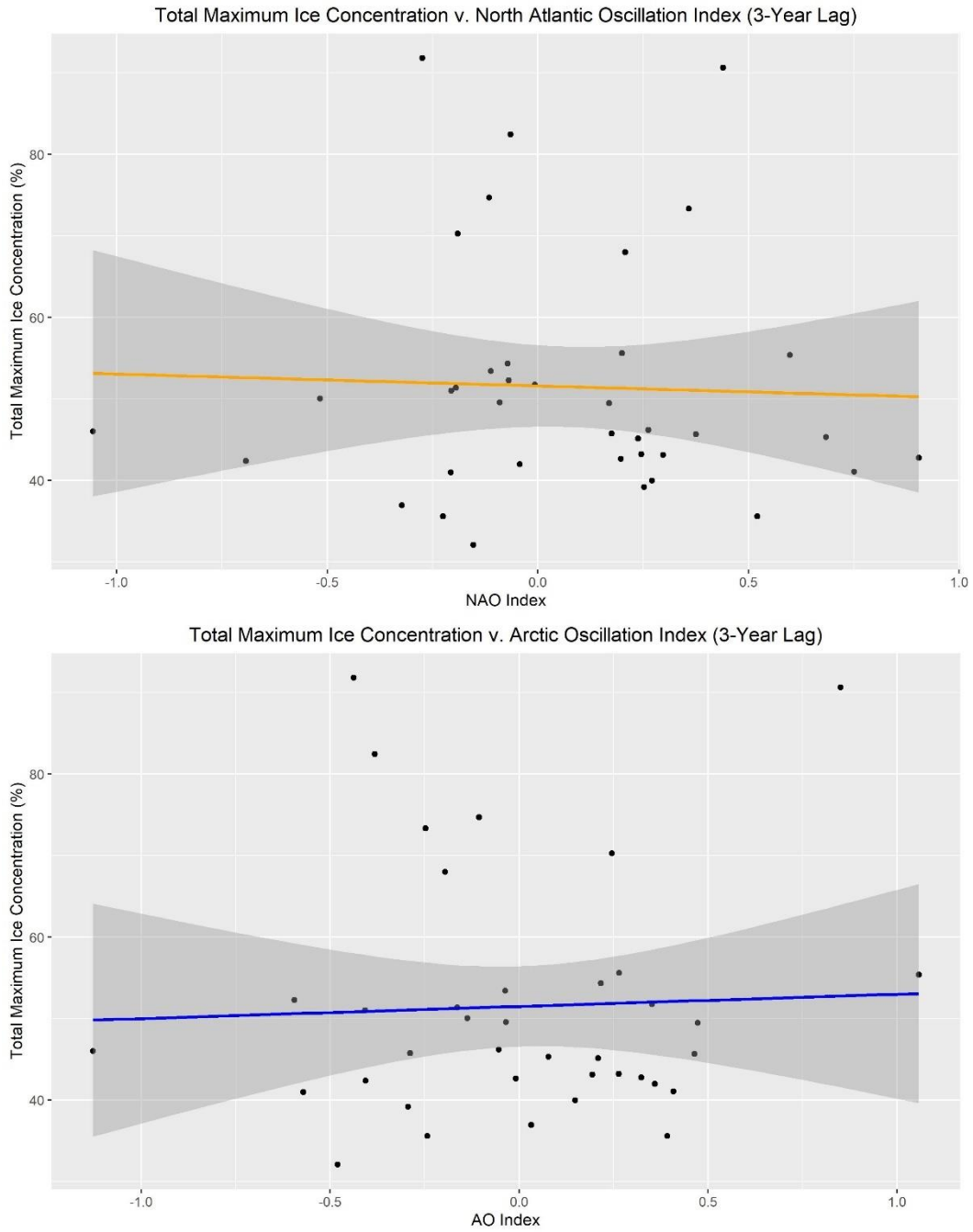


Figure 4.1(d) 3-Year Linear Regression plot of NAO (Top), AO (Bottom) and Total Maximum Sea Ice Coverage in Northern Labrador. Grey Area denotes 95% CI.

NAO:  $r = -0.03$ ,  $p=0.817$ ,

AO:  $r = 0.0426$ ,  $p=0.799$

Figure 4.4(a) Sea Ice Maximum v. I48Ns (0-Year Lag)

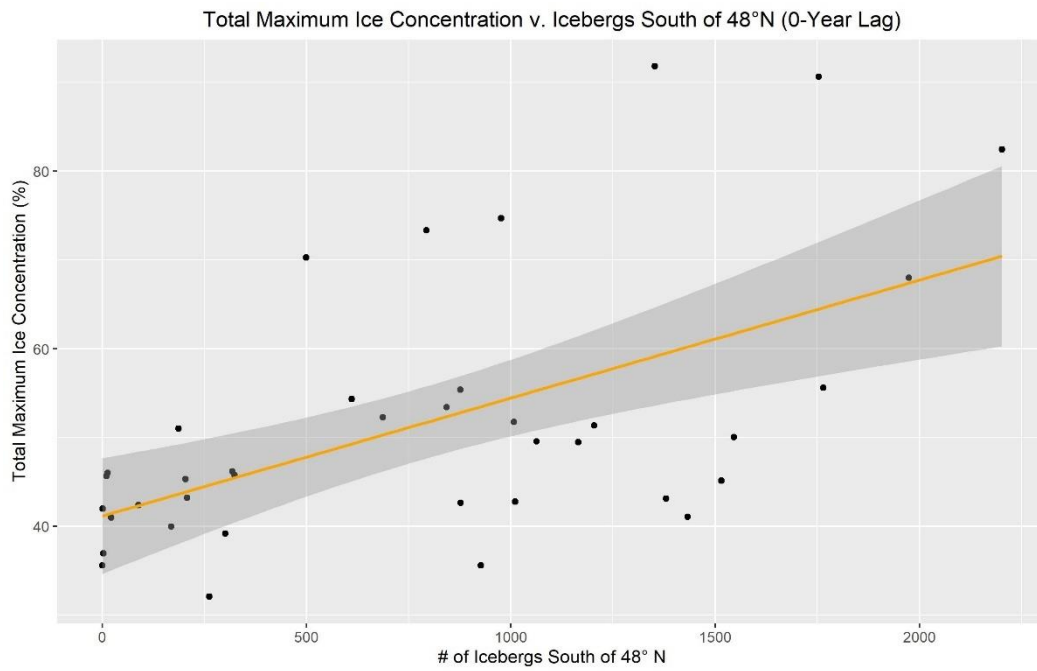


Figure 4.4(a) 0-Year Linear Regression plot of Total Maximum Sea Ice Coverage in Northern Labrador and Number of Icebergs detected South of 48°N. Grey Area denotes 95% CI. Bold denotes significance.

**$r = 0.5664, p=0.00021$**

Figure 4.4(b) Sea Ice Maximum v. I48Ns (1-Year Lag)

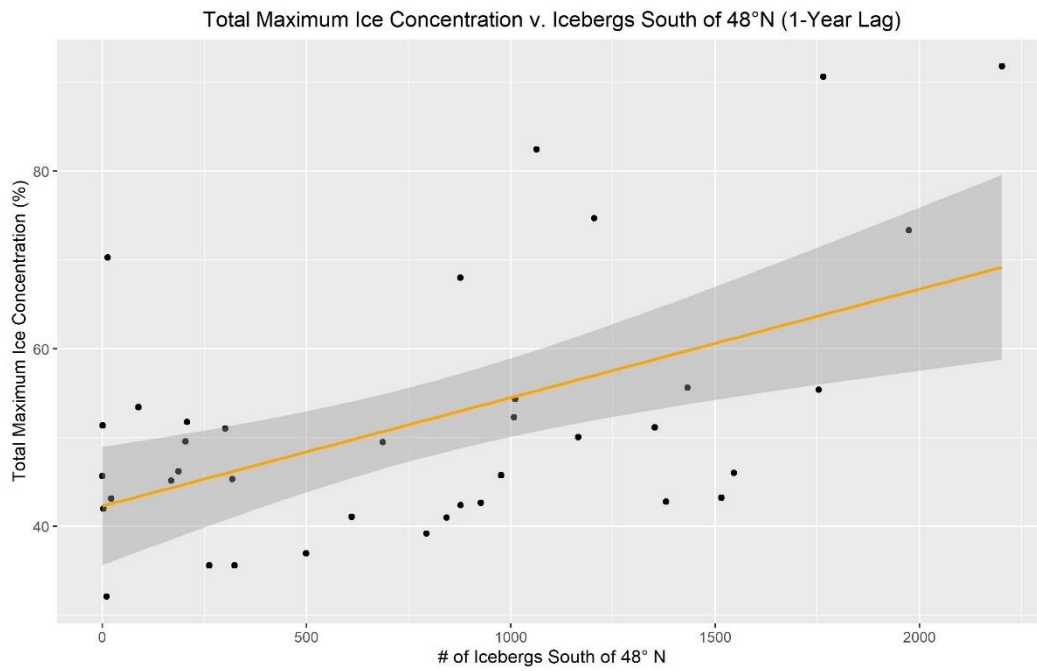


Figure 4.4(b) 1-Year Linear Regression plot of Total Maximum Sea Ice Coverage in Northern Labrador and Number of Icebergs detected South of 48°N. Grey Area denotes 95% CI. Bold denotes significance.

**$r = 0.5252$ ,  $p=0.00071$**

Figure 4.4(c) Sea Ice Maximum v. I48Ns (2-Year Lag)

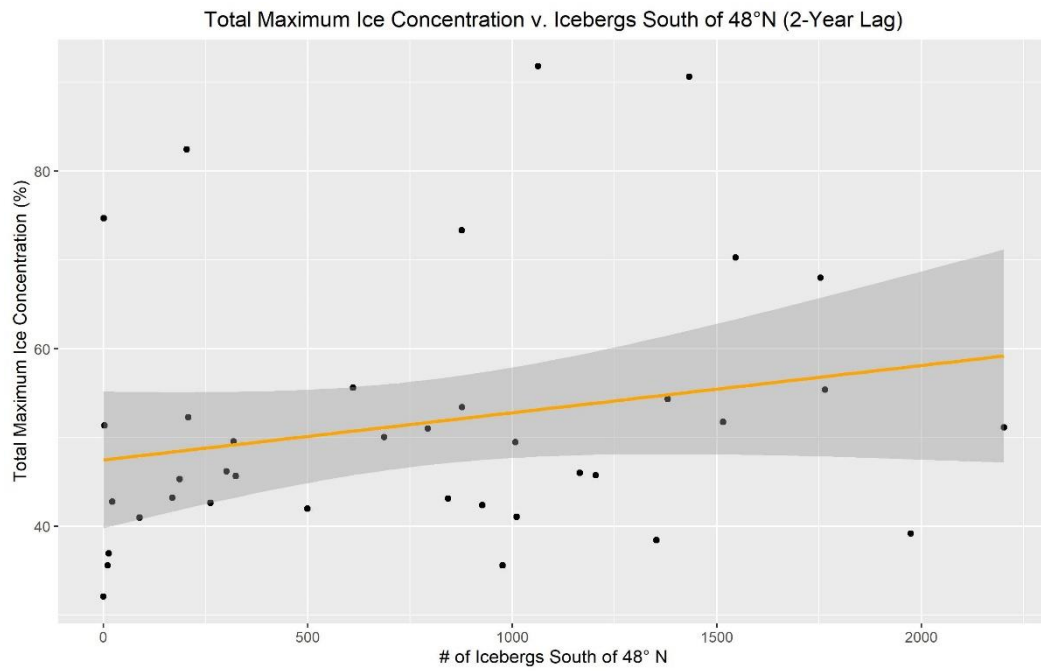


Figure 4.4(c) 2-Year Linear Regression plot of Total Maximum Sea Ice Coverage in Northern Labrador and Number of Icebergs detected South of 48°N. Grey Area denotes 95% CI.

$r = 0.226$  ,  $p = 0.171$

Figure 4.4(d) Sea Ice Maximum v. I48Ns (3-Year Lag)

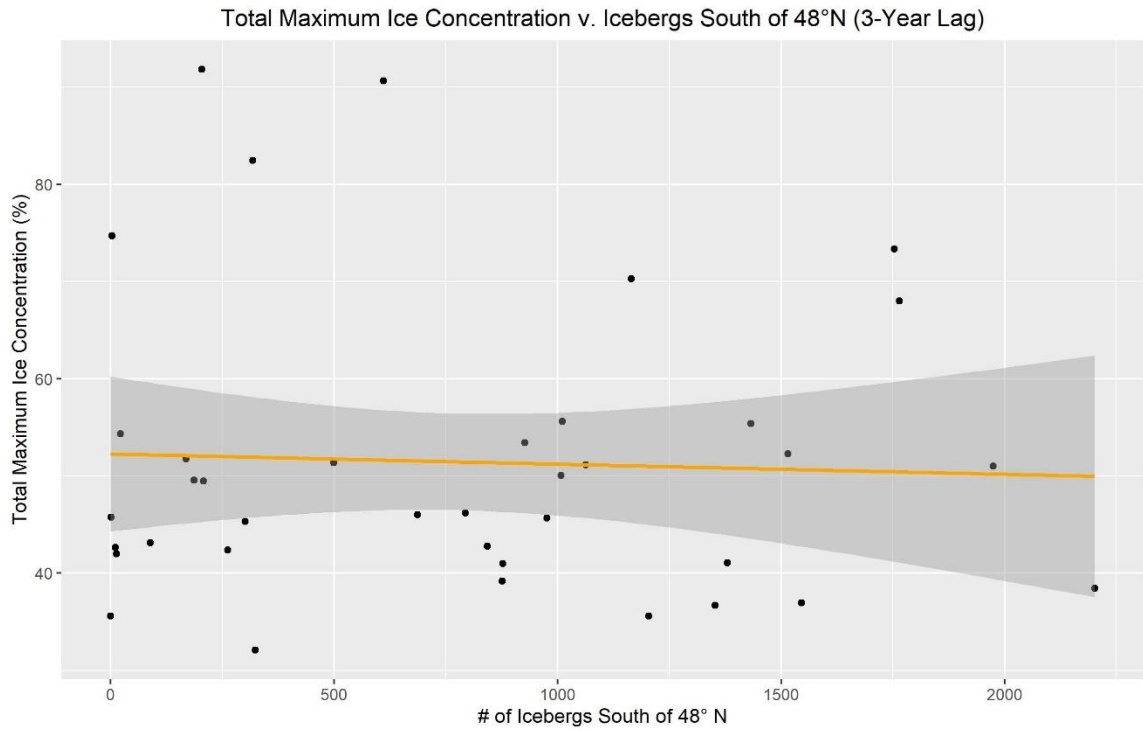


Figure 4.4(d) 3-Year Linear Regression plot of Total Maximum Sea Ice Coverage in Northern Labrador and Number of Icebergs detected South of 48°N. Grey Area denotes 95% CI.

$$r = -0.044, p=0.7922$$

# Geopotential Height (500hPa)

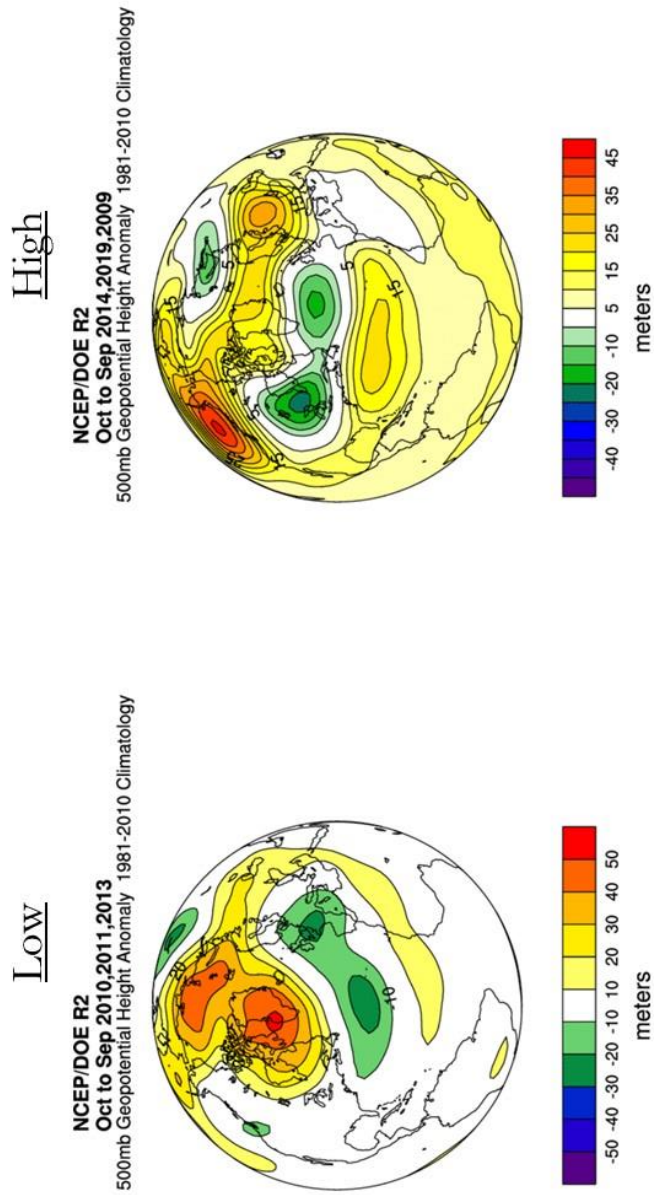


Figure 4.6.1

Reanalysis, Geopotential Height

Figure 4.6.1: NCEP/DOE Reanalysis II Plot, Geopotential Height Anomaly (500 hPa) in Low (Left) and High (Right) Iceberg years. Based on 1981-2010 Climatology.

# Relative Humidity

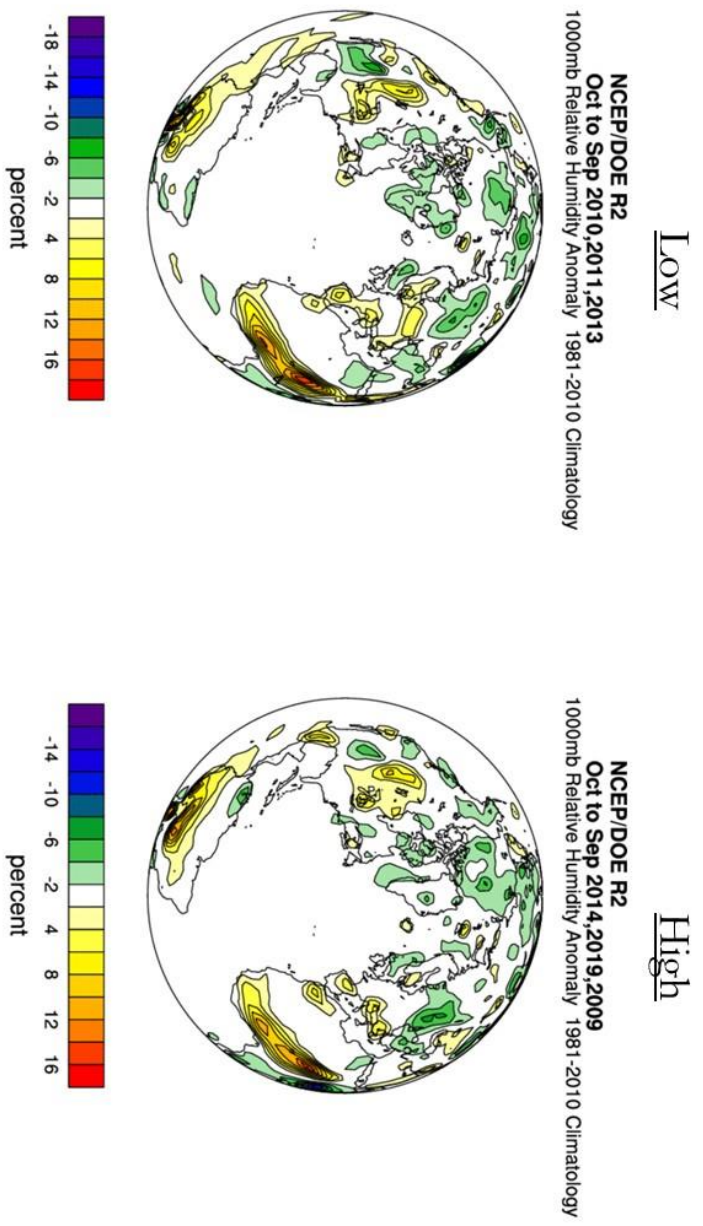


Figure 4.6.2: NCEP/DOE Reanalysis II Plot, Relative Humidity Anomaly in Low (Left) and High (Right) Iceberg years. Based on 1981-2010 Climatology.

Figure 4.6.2  
Reanalysis, Relative Humidity

Figure 4.6.3  
Reanalysis, Omega

# Omega

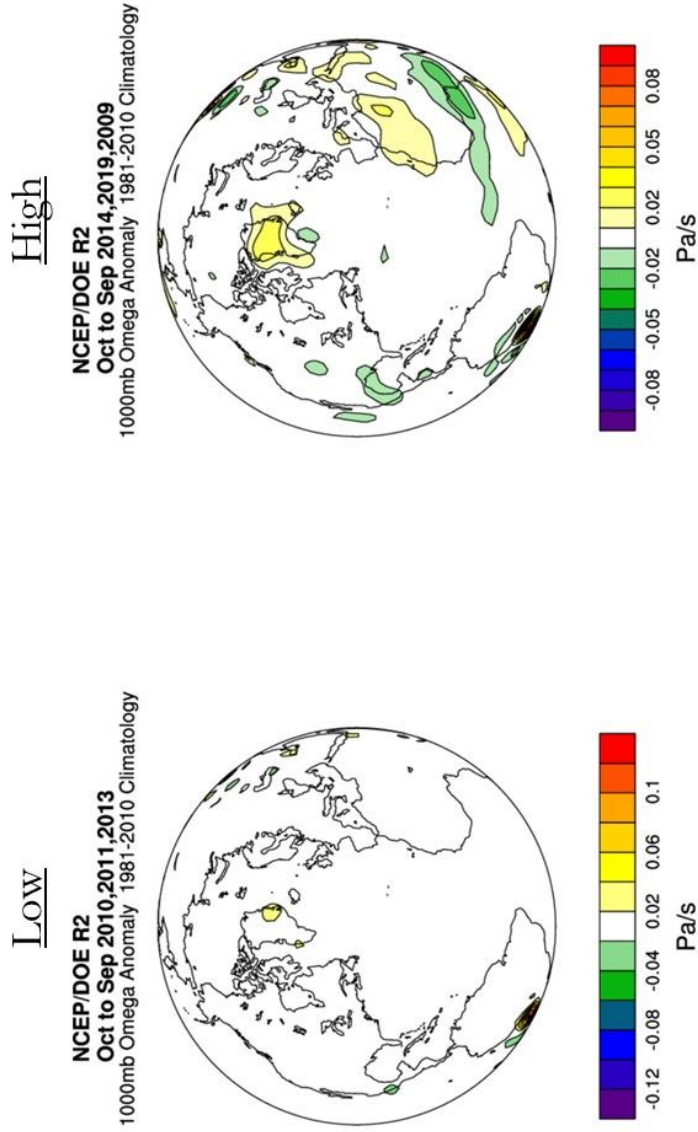


Figure 4.6.3: NCEP/DOE Reanalysis II Plot, Omega anomaly in Low (Left) and High (Right) Iceberg years. Based on 1981-2010 Climatology.

# Sea Ice

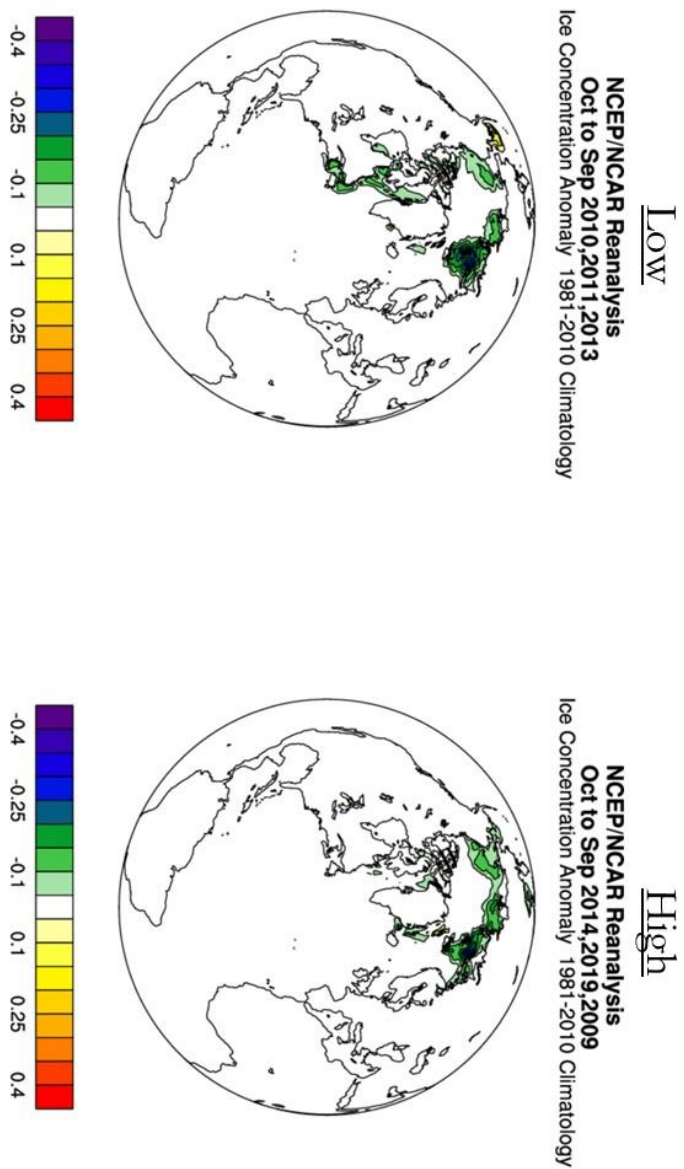


Figure 4.6.4: NCEP/NCAR Reanalysis Plot, Sea Ice Anomaly in Low (Left) and High (Right) Iceberg years. Based on 1981-2010 Climatology. Measured in Percent Coverage

Figure 4.6.4  
Reanalysis, Sea Ice

# Sea Level Pressure

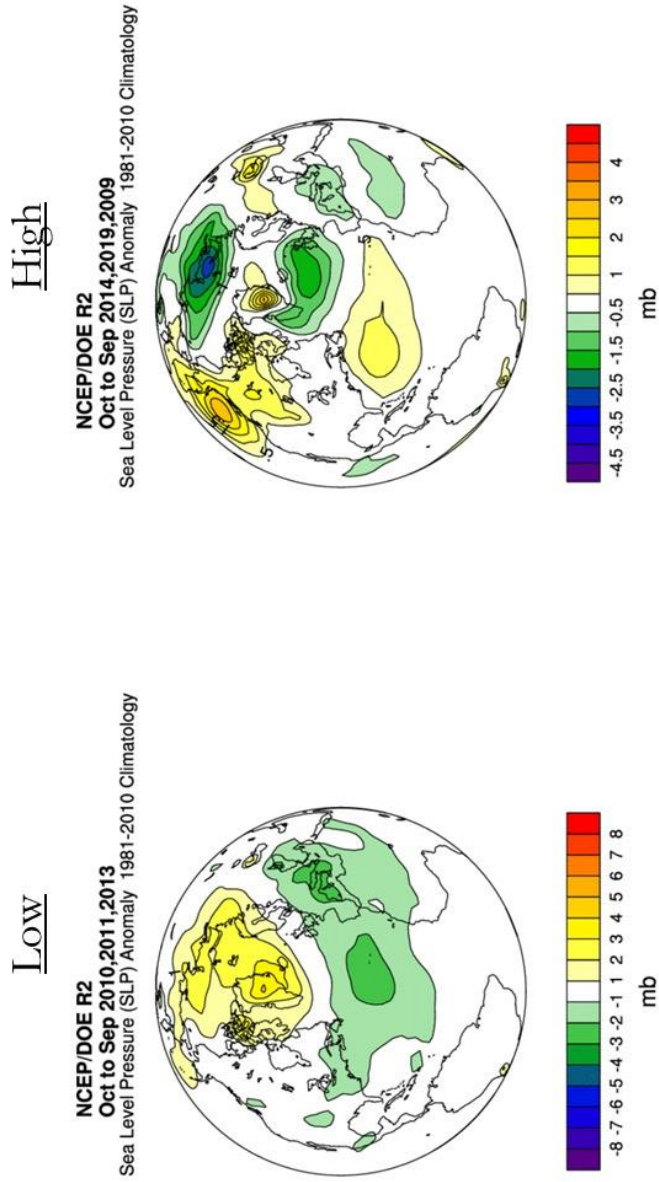


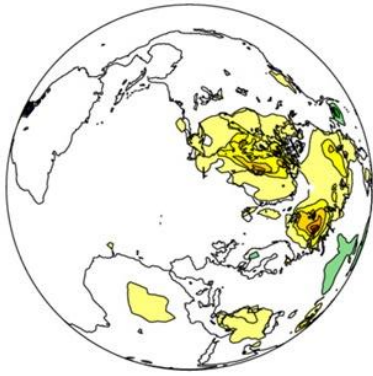
Figure 4.6.5  
Reanalysis, Sea Level Pressure

Figure 4.6.5: NCEP/DOE Reanalysis II Plot, Sea Level Pressure Anomaly in Low (Left) and High (Right) Iceberg years. Based on 1981-2010 Climatology.

# Skin Temperature / SST

Low

NCEP/NCAR Reanalysis  
Oct to Sep 2010,2011,2013  
Sea Surface/Skin Temp Anomaly 1981-2010 Climatology



High

NCEP/NCAR Reanalysis  
Oct to Sep 2014,2019,2009  
Sea Surface/Skin Temp Anomaly 1981-2010 Climatology

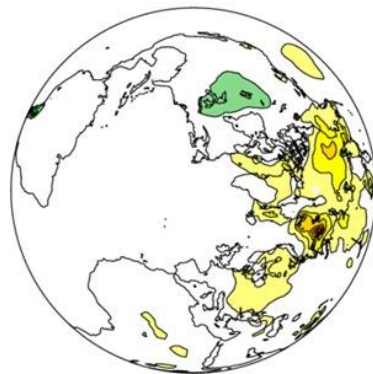


Figure 4.6.6  
Reanalysis, SST/Skin Temperature

Figure 4.6.6: NCEP/NCAR Reanalysis Plot, Skin Temperature/SST in Low (Left) and High (Right) Iceberg years. Based on 1981-2010 Climatology.

# Air Temperature

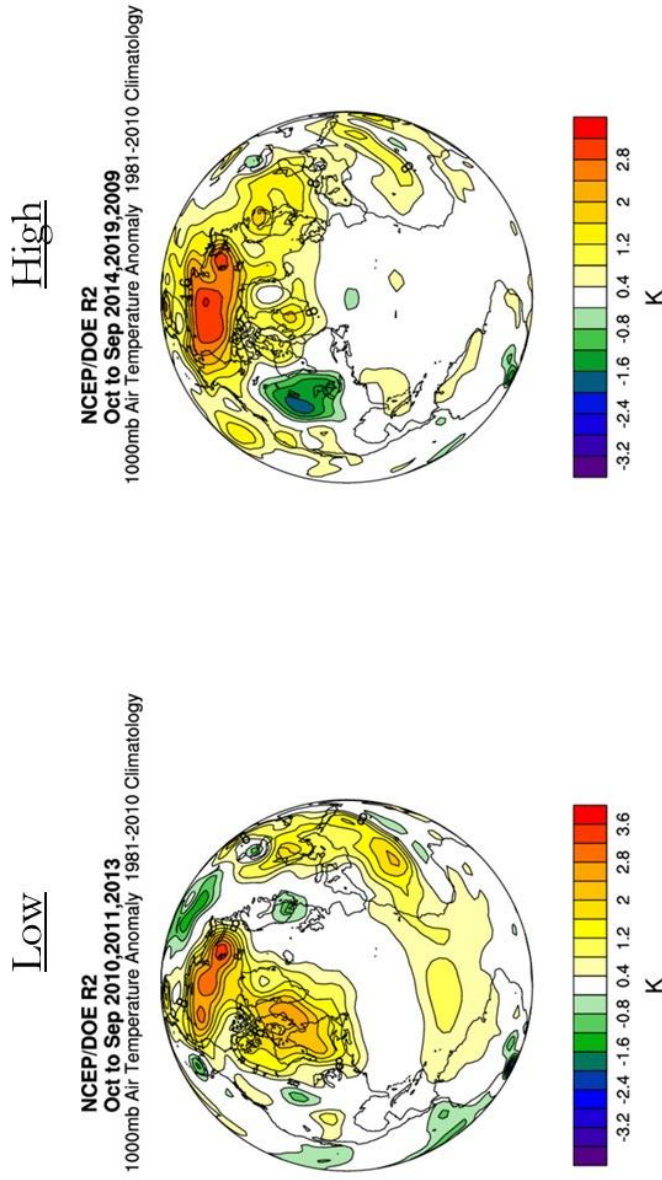


Figure 4.6.7  
Reanalysis, Air Temperature

Figure 4.6.7: NCEP/DOE Reanalysis II Plot, Air Temperature Anomaly in Low (Left) and High (Right) Iceberg years. Based on 1981-2010 Climatology.

# Zonal Wind

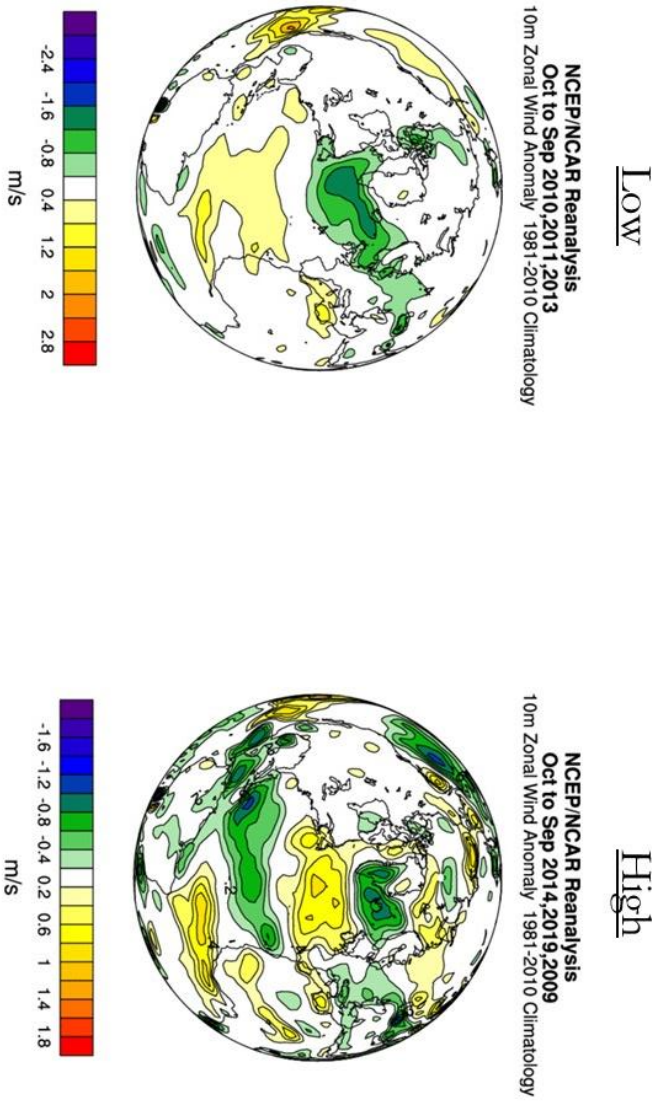


Figure 4.6.8  
Reanalysis, Zonal Wind

Figure 4.6.8: NCEP/NCAR Reanalysis Plot, Zonal Wind Anomaly in Low (Left) and High (Right) Iceberg years. Based on 1981-2010 Climatology. Positive values are associated with southerly winds, negative values are associated with northerly winds

# Meridional Wind

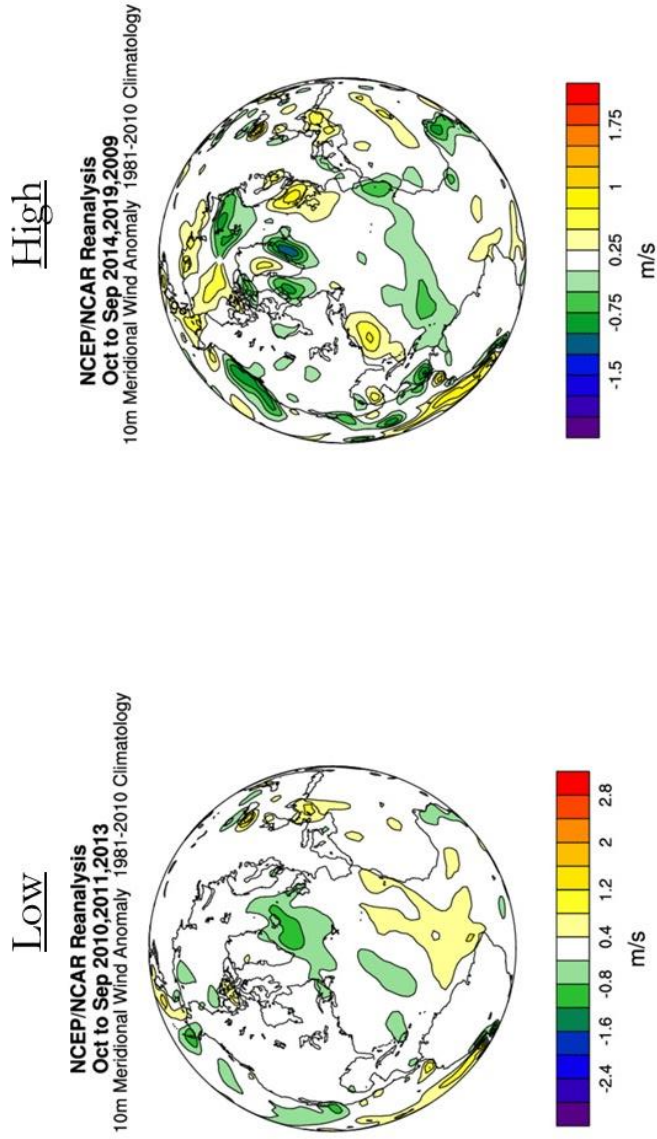


Figure 4.6.9: NCEP/NCAR Reanalysis Plot, Meridional Wind Anomaly in Low (Left) and High (Right) Iceberg years. Based on 1981-2010 Climatology. Positive values are associated with westerly winds, negative values are associated with easterly winds

Figure 4.6.9  
Reanalysis, Meridional Wind

Table 4.1

**Linear Regressions, North Atlantic Oscillation**

Predictor Variable: Number of Icebergs South of 48° N

Response Variable: North Atlantic Oscillation Index

Lag	r	R <sup>2</sup>	Estimate	Std. Er.	t-value	p-value	df1/df2	F
0-year	0.1559	0.02431	235.5	248.6	0.947	0.3499	1/36	0.8971
<b>1-year</b>	<b>0.4341</b>	<b>0.1885</b>	<b>653.9</b>	<b>226.1</b>	<b>2.892</b>	<b>0.00646</b>	<b>1/36</b>	<b>8.361</b>
2-year	0.1623	0.02637	245.9	249.0	0.987	0.3301	1/36	0.9749
3-year	0.2446	0.05985	392.8	259.4	1.514	0.1388	1/36	2.292

**Note: Statistical significance denoted by bold text.**

Table 4.2

**Linear Regressions, Arctic Oscillation**

Predictor Variable: Number of Icebergs South of 48° N

Response Variable: Arctic Oscillation Index

Lag	r	R <sup>2</sup>	Estimate	Std. Er.	t-value	p-value	df1/df2	F
0-year	0.2017	0.0407	344.0	239.8	1.434	0.1601	1/36	2.058
<b>1-year</b>	<b>0.3432</b>	<b>0.1178</b>	<b>524.08</b>	<b>239.04</b>	<b>2.192</b>	<b>0.0349</b>	<b>1/36</b>	<b>4.807</b>
2-year	0.2622	0.0688	396.0	242.8	1.631	0.1116	1/36	2.66
3-year	0.2488	0.06192	372.2	241.4	1.542	0.132	1/36	0.1319

**Note: Statistical significance denoted by bold text.**

Table 4.3

**Logistic Regressions**

Predictor Variable: Number of Icebergs South of 48° N

148N Cat.	Model	Estimate	Std. Er.	Z Value	P value	AIC	95% CI
Light	NAO	-1.6624	0.9966	-1.668	0.0953	46.499	-3.891, 0.142
	AO	-1.4563	0.9767	-1.491	0.136	47.245	-3.595, 0.341
Light	Both(N)	-1.2468	1.2914	-0.965	0.3343	48.255	-4.01, 1.164
	Both(A)	-0.6287	1.2808	-0.491	0.6235	48.255	-3.281, 1.845
Moderate	NAO	-0.1122	0.8045	-0.139	0.889	54.963	-1.742, 1.501
	AO	0.1867	0.8187	0.228	0.82	54.93	-1.439, 1.866
Moderate	Both(N)	-0.4155	1.0804	-0.385	0.701	56.781	-2.628, 1.696
	Both(A)	0.463	1.0875	0.426	0.67	56.781	-1.686, 2.661
Heavy	NAO	-1.0069	1.1652	-0.864	0.3874	32.997	-3.455, 1.277
	AO	0.1559	1.1838	0.132	0.895	33.575	-2.166, 2.567
Heavy	Both(N)	-2.3375	1.8927	-1.235	0.2168	33.777	-6.689, 0.985
	Both(A)	1.7149	1.7147	1.000	0.3172	33.777	-1.528, 5.491
Extreme	NAO	<b>4.3674</b>	<b>1.6867</b>	<b>2.589</b>	<b>0.009616</b>	<b>29.509</b>	<b>1.551, 8.418</b>
	AO	1.5744	1.144	1.376	0.168774	38.217	-0.537, 4.094
Extreme	Both(N)	<b>4.8562</b>	<b>1.9991</b>	<b>2.429</b>	<b>0.01513</b>	<b>31.245</b>	<b>1.507, 9.722</b>
	Both(A)	-0.7808	1.5322	-0.51	0.610332	31.245	-4.063, 2.23

**Note: Statistical significance denoted by bold text.**

Both(N) = Coefficients for NAO in Combination Model

Both(A) = Coefficients for AO in Combination Model

Table 4.4

**AIC Testing**

Model	K	AICc	Delta AICc	AICc Wt.	Cum. Wt.	LL
NAO Only	4	99.60	0.00	0.39	0.39	-45.67
NAO - AO	4	99.60	0.00	0.39	0.78	-45.67
NAO + AO	5	101.74	2.14	0.13	0.91	-45.66
NAO x AO	6	103.90	4.29	0.05	0.96	-45.66
AO Only	4	104.03	4.43	0.04	1.00	-47.88

Table 4.5

**Linear Regressions, NAO v. Sea Ice**

Response Variable: NAOI v. Sea Ice Maximum

Lag	R	R <sup>2</sup>	Estimate	Std. Er.	t-value	p-value	df1/df2	F
0-year	0.2266	0.051	0.006394	0.00457	0.397	0.171	1/36	1.95
1-year	0.2755	0.075	0.0077	0.00453	1.720	0.094	1/36	2.958
2-year	-0.111	0.0125	-0.0031	0.00466	-0.676	0.503	1/36	0.4572
3-year	-0.03	0.0015	-0.0010	0.00442	-0.233	0.817	1/36	0.05424

**Note: Statistical significance denoted by bold text.**

Table 4.6

**Linear Regressions, AO v. Sea Ice**

Response Variable: AOI v. Sea Ice Maximum

Lag	R	R <sup>2</sup>	Estimate	Std. Er.	t-value	p-value	df1/df2	F
0-year	0.2310	0.533	0.0066	0.00467	1.525	0.163	1/36	2.031
<b>1-year</b>	<b>0.3891</b>	<b>0.1515</b>	<b>0.0108</b>	<b>0.00428</b>	<b>2.535</b>	<b>0.0157</b>	<b>1/36</b>	<b>6.427</b>
2-year	-0.055	0.0031	-0.0016	0.00469	-0.332	0.742	1/36	0.1102
3-year	0.0426	0.0018	0.0012	0.00474	0.256	0.799	1/36	0.0655

**Note: Statistical significance denoted by bold text.**

Table 4.7

**Linear Regressions, Sea Ice v. I48Ns**

Response Variable: Sea Ice Maximum vs. I48Ns

Lag	R	R <sup>2</sup>	Estimate	Std. Er.	t-value	p-value	df1/df2	F
<b>0-year</b>	<b>0.5664</b>	<b>0.3208</b>	<b>24.128</b>	<b>5.851</b>	<b>4.124</b>	<b>0.00021</b>	<b>1/36</b>	<b>17.01</b>
<b>1-year</b>	<b>0.5252</b>	<b>0.2758</b>	<b>22.563</b>	<b>6.093</b>	<b>3.703</b>	<b>0.00071</b>	<b>1/36</b>	<b>13.71</b>
2-year	0.226	0.051	9.661	6.916	1.397	0.171	1/36	1.951
3-year	-0.044	0.0002	-1.865	7.028	-0.265	0.7922	1/36	0.0704

**Note: Statistical significance denoted by bold text.**

## 5. DISCUSSION

### 5.1 Discussion of Lag Models

Of the four temporal lags tested by linear regression, the 1-year lag has the strongest correlation between both NAO and AO when correlated with number of I48Ns. This result is mostly expected, as the NAO or AO Index values from one year would be unlikely to impact the number of I48Ns within the same year (0-year lag), due to the transit time needed for an iceberg to travel from Greenland to the 48<sup>th</sup> Parallel. Due to the statistical significance of the 1-year lag, this lag period is used for subsequent statistical analyses, including Logistic regressions and AIC testing. Given this result, the question is which meteorological and/or oceanographic factors are the NAO and AO driving in the North Atlantic and Arctic that would result in a correlation with I48Ns at this lag, as opposed to others. The likelihood of some interaction along the transit path of I48Ns that influences that transit is likely. This topic is explored further in sections 3.6 and 4.6, regarding case studies.

The 2-year and 3-year lags are notably also not significant in this case. This result further solidifies that the critical period of influence of the NAO and AO as drivers of I48N counts occurs during the preceding year.

### 5.2 Discussion of Logistic Regression Modeling

While the logistic regression analysis has only two statistically significant models, some interesting numerical patterns emerge when examining the results as a whole. This is most visible when examining Figure 4.2. In each of the three models (NAO, AO, NAO/AO) the influence of these teleconnections is concentrated at the tails of the severity categories. There is a much higher probability of a Light iceberg year when the NAO and AO Indices for the previous year are also low, negative in this case. Similarly, probability of an Extreme iceberg year is much higher when the NAO and AO Indices are higher. The

influence of these teleconnections is not as strong in the middle iceberg severity categories (Moderate, Heavy) Moderate ice years have occurred expectedly in the middle of the NAO/AO distribution. All instances of a moderate iceberg year since 1983 have occurred when the NAOI was between -0.5 and 0.6. The AO driven distribution of Moderate iceberg years is much larger, with moderate icebergs observed in years with AOI values between -.04 and 1.05. The year 1990, with an AOI value of 1.05, occurred when the AO index was at its highest for the entire period of record (1983-2020), this and other exceptions speak to the fact that NAO and AO are not the only driving factor in I48N counts.

Within the statistically significant NAO on Extreme iceberg count models, there are some notable exceptions. For instance, the years 1994 and 2014 with NAOI values of -0.07 and -0.06, were extreme iceberg years, despite being outliers from the high NAO/high iceberg pattern. Similarly, 2001, a year with an NAO index of 0.52, which is among other common NAOI values for other extreme years is a light iceberg year. These outlier iceberg years are counterintuitive, and their causes present a gap worth continued research.

Estimates for these models (Table 4.3) confirm a similar pattern of concentrated influence in the Light and Extreme iceberg categories. Estimates for Light Icebergs across all three models are strongly negative, suggesting higher probability of a Light year with negative NAO/AO, while similarly estimates for the Extreme category are strongly positive across all models, significantly so in the case of NAO. The Heavy and Moderate categories are not as broadly described, both the Heavy and Moderate Estimates are closer to zero on the NAOI distribution, while remaining slightly negative. For AO, the case is opposite, with estimates slightly on the positive side of the AOI distribution. This suggests that there is more variability when Heavy and Moderate ice years can occur with respect to these

teleconnections. With the strength of Light and Extreme categories in the ability of NAO and AO to predict the presence of a given year in one of these tail-end categories broadly shows that a pattern emerges where light iceberg years are more likely to follow a year when the NAO and AO indices are negative, while extreme iceberg years are more likely when NAO and AO are strongly positive.

### **5.3 Discussion of AIC Testing of Model Fit**

Based on the quantified advantage in correlation and probability of the NAO in comparison to the AO in the results of previous analyses, it became apparent that the NAO and the AO needed to be tested for model fit. Given that thus far the NAO has been the stronger variable, the AIC model test was designed to test the strength of multivariate regression models by increasing the influence of AO across multiple models, and examining the change in model fitness. The results of this test (Table 4.4) are in line with the results of previous tests. As the influence of AO in the model increases, the fitness of the model becomes progressively weaker. The AIC of a model quantifies model fit, in this case is ordered from best fit (lowest AIC) to worst fit (highest AIC). With this group of models, this best-to-worst fit order also follows least-to-most influence of AO. The strongest models are the NAO only model, with no AO influence and the subtractive model (NAO – AO). Both with AIC of 99.60, and an AIC weight of .39. These models capture 39% of the variation in the entire dataset. The additive model (NAO + AO) is the next weakest model and represents an increase in the influence of AO in the model. This model has an AIC of 101.74, however, the AIC weight is 0.13, a marked decrease in the amount of variation explained from the previous model. The next weakest model is the multiplicative model (NAO x AO), with an AIC of 103.90, and only 5% of the variation in I48Ns explained. Finally, the weakest model is the AO only model, with the most AO influence, as it is the

only variable. The model had an AIC of 104.03 and explains just 4% of the variation in I48N counts. The result of this analysis is that between AO and NAO, the North Atlantic Oscillation has the stronger influence of the two teleconnections as a driver for I48Ns.

As the North Atlantic Oscillation is a regional manifestation of the Arctic Oscillation, this raises questions regarding the nature of this relationship in the North Atlantic, and the influence of each on I48Ns.

#### **5.4 NAO/AO as Driver of Sea Ice Extent**

Sea Ice is an important factor in the transit of icebergs. Icebergs along the Labrador shelf act as a buffer, preventing icebergs from stranding in the shallows and failing to progress to the North Atlantic. However, as previous analysis within this work have determined a strong link between Arctic Teleconnections (especially the NAO) and the number of I48Ns detected in a given ice year, it is also important to examine the relationship between these teleconnections and sea ice in the Labrador Sea. In examining NAO/AO correlation with Sea Ice Maximum Percentage at the trend to this point of NAO being the stronger influence is overturned. There were no statistically significant correlations between sea ice maximum and NAOI at 0-, 1-, 2-, and 3-year lags. When using AOI as a predictor variable, there is significant correlation with Sea Ice Maximum as a response at a 1-year lag. This relationship's coefficient of determination of 0.1515 indicates that AO is responsible for 15% of the variation in sea ice maximum percentage. This strength of the AO over the NAO in this analysis warrants future study, as the results are not in line with analyses up to this point. This finding also indicates that there are other influences between NAO and I48Ns other than sea ice which need identification and study. Additionally, given the limited space of sea ice data in Northern Labrador leaves opportunity for additional testing of

teleconnections as a driver for sea ice along greater areas of the Labrador Shelf, as well as across the Labrador Sea and Davis Strait.

### **5.5 Sea Ice Maximum as a Driver of I48Ns**

Given the evidence of a complex relationship between arctic teleconnections, sea ice, and I48Ns present in the data and analysis, it is imperative to examine the impact of sea ice as a direct influence on the number of I48Ns, to shed some light on the inconsistencies between Teleconnection-Ice and Teleconnection-Iceberg relationships. This analysis was again conducted at 0-, 1-, 2- and 3-year lags, and found that sea ice maximum percentage and resulted in statistically significant correlation between I48Ns and sea ice maximum percentage at 0- and 1-year lags. These moderately strong correlation coefficients (0-year: 0.5664, 1-year: 0.5252) at these lags indicate that it is possible for icebergs to transit from Northern Labrador to the 48<sup>th</sup> Parallel within 0-1 ice years. It is also possible that icebergs can survive for at least 1 year in the area between Northern Labrador and the 48<sup>th</sup> Parallel. In order to determine whether these lags being significant is the result of >1 year transit, or iceberg survivability, would require in-situ observation of iceberg transit. Given the coefficients of determination (0-year: 0.3208, 1-year: 0.2758), two main conclusions can be reached. First, sea ice maximum in Northern Labrador drives a higher percentage of I48N variability in the same ice year, rather than the subsequent ice year. Second, that with ~70% of variability in I48Ns not explained by this model, coupled with the weak correlation between AO/NAO and Sea Ice indicates that other oceanographic/meteorological factors are unaccounted for in describing the number of I48Ns detected in a given ice year, and the influence of AO/NAO on those factors. Additionally, as mentioned in section 5.4, expanding the sea ice data field to the entire Labrador shelf and Davis Straight could provide further detail in the description of these relationships.

## 5.6 Discussion of Case Studies

Of the case study results reported in section 4.6, there are some categories in which the difference between conditions in Low and High Iceberg years warrant further discussion, being Geopotential Height, Sea Ice, Sea Level Pressure, and Sea Surface/ Skin Temperature ( $SST_{skin}$ ).

While examining geopotential height, an interesting pattern emerges. In low iceberg years, the atmospheric setup of the 500hPa height field matches with the loading pattern of the negative phase of the NAO outlined by Thompson and Wallace (1998). This is in line with results of both Linear and Logistic regression analyses. The linear regression analysis determines statistically significant correlation with I48Ns on a 1-year lag. The logistic regression, while not statistically significant, does show a trend in likelihood of light icebergs being more likely with strongly negative AO. The height field setup during the high iceberg years is not consistent with either high or low AO and may represent a transitional phase. Additionally, the adjacency of the low iceberg years (2010, 2011, 2013) compared to the more distant high iceberg years (2014, 2019, 2009) may have resulted in a less consistent height field pattern in the reanalysis of the high iceberg years.

Sea Ice, while examined statistically in this work, when examined in the context of reanalysis opens some interesting possibilities. The lower-than-normal sea ice anomalies during the low iceberg years across the Labrador shelf and across Davis Strait into Baffin Bay indicates a spatially large area in which sea ice conditions can impact the transit of an I48N. While the statistical analysis of sea ice contained in this work is focused on the northern Labrador coast, and therefore has the strongest correlation with I48Ns at the 0- and 1-year lags, sea ice analysis closer to Greenland has the possibility to carry very different results.

Sea Level Pressure values as depicted in figure 4.6.6, are consistent with NAO phases. During low iceberg years, The Azores High is weaker than the climatological normal, and the Icelandic Low is stronger than normal. This reflects the covariation in this pressure system present in the negative phase of the NAO, which has been determined in this study through statistical analysis to have a greater likelihood of a low iceberg year. In the high iceberg years, the Icelandic Low and Azores high are both stronger, consistent with the positive phase of the NAO. This is consistent with the NAOI means for these years with a low iceberg year NAOI mean of -0.47 and a high iceberg mean of -.15, While both are negative index values, the high iceberg years have a higher NAOI value. This observation does support the results present in previous sections.

Finally, Sea Surface/ Skin Temperature has some notable similarities between the low and high iceberg years, namely higher-than-normal temperatures in Baffin Bay. However, during the low ice years, these higher-than-normal temperatures are much higher than both the climatological normal, and the high iceberg years. Additionally, the low iceberg years have a greater area of above normal temperatures, extending the full path of iceberg transit from West Greenland, to the 48<sup>th</sup> Parallel in Newfoundland. The broad possibilities for impacts of warmer seas on icebergs over such large area, as well as unexplained variability in previous statistical analyses lends itself to further study of sea surface temperatures.

## 6. CONCLUSION

### 6.1 Summary

This study has been conducted to build on research produced by the International Ice Patrol (Rudnickas and Serumgard, 2018), with the goal of better understanding the influence of the Arctic Oscillation and the North Atlantic Oscillation on the presence of icebergs observed south of 48°N. This study has resulted in five key findings that have achieved this goal and provided future direction in the broader goal of developing an iceberg forecasting system to be utilized by the IIP. The first key finding resulting from this study is that the both the Arctic Oscillation and the North Atlantic Oscillation have a statistically significant correlation with the number of icebergs detected south of 48° N on a 1-year lag, through the use of simple linear regression. The isolation of this lag time allowed for the strongest influence of these teleconnections to be more specifically examined. This finding not only temporally isolates the influence of these teleconnections on I48Ns but does so spatially as well. With the IIP estimating that the usual transit time for an iceberg to reach the North Atlantic is between one and three years (IIP 2016; IIP 2018), this influence being significant suggests that NAO and AO more strongly influence an iceberg that is undergoing transit, rather than the calving process in the early life of an iceberg.

Using logistic regression to examine more closely the previously determined one year lag time, and the influence of teleconnections on I48N presence resulted in the second key finding. Strongly positive NAO Index values are linked to an increased likelihood of an extreme iceberg year the following year. While the NAO values were statistically significant only when predicting the likelihood of extreme iceberg years, a trend emerges with both NAO and AO values. The influence of these teleconnections on I48Ns is concentrated at the tails of the distribution. (Figure 4.2a-c), with strongly negative AOI and NAOI values

increasing the likelihood of a light ice year following, and strongly positive AOI and NAOI increasing the likelihood of an extreme iceberg year following. The probability of a moderate or heavy iceberg year is not strongly linked to either positive or negative NAO or AO values. This is likely owing to the fact that there are some outliers, in which NAO and/or AO Value are high enough for there to be a strong likelihood of an extreme iceberg year, yet one does not follow. The same is true in the inverse, there are some Extreme icebergs years that were not preceded by high NAO/AO values. While the probability of the following year's number of icebergs is strongly linked to the NAO/AO values for the previous year there is unaccounted for variability that thus far prohibit using only NAO and/or AO to forecast the number of I48Ns with any real precision.

The previous analyses followed a common trend, where NAO has been the statistically stronger influence on the number of I48Ns. This led to testing models of variable AO influence to determine if the strength of the models decreased with greater AO influence, as is suggested in previous analyses. The testing of the Akaike's Information Criterion (AIC) led to the third key finding, that when it comes to direct influence of NAO/AO on the number of I48Ns observed, NAO is the stronger driver. This test confirmed the findings of previous analyses within this work.

With the previous three key findings relating to direct influence of Arctic teleconnections on North Atlantic Icebergs, sea ice is examined both as a driver of I48Ns, and as a response to NAO and AO. It is in this stage that the superiority of NAO as an influence to this point is overturned. As AO is more strongly linked to sea ice maximum percentage in Northern Labrador, with significant correlation in simple linear regression at a 1-year lag. This result is based on ice data from a coastal area in Northern Labrador, and it is

unclear if expansion of sea ice maximum inclusion to the entirety of the Labrador Shelf, would yield the same results.

The final key finding comes as a result of examining the influence of this Northern Labrador Sea ice on I48Ns. The maximum sea ice percentage strongly correlates with the number of I48Ns on both 0- and 1-year lags. This result is in line with IIP's current understanding (IIP, 2016; IIP, 2018) that coastal sea ice in Labrador acts as a buffer that allows icebergs to cross the Labrador Sea without stranding. Interestingly, this is the only instance in the study of a significant correlation between a driver and I48Ns at a 0-year lag. This finding indicates that icebergs in northern Labrador are able to transit past the 48<sup>th</sup> Parallel, within the same ice year.

## **6.2 Future Research**

Future work can largely be divided into three categories, inclusion of additional variables, expanded statistical analysis, and in-situ data collection. Inclusion of these categories is directed towards the goal of developing a reliable iceberg forecasting system to be operated by the International Ice Patrol.

Inclusion of additional variables is informed both by suggestions devised by Rudnickas and Serumgard (2018), as well as by the results of the Case Studies in this work. Sea ice (Marko et al., 1994; Rudnickas and Serumgard, 2018), coastal glacier calving in Southwest and Southeast Greenland (Bigg et al., 1999, Bigg et al., 2014) and/or ocean currents (Yashayaev, 2007; Fischer et al. 2010; Palter et al., 2016; Yang et al., 2021) are strong candidates for I48N drivers, and these previous works can be combined to better understand the influence of each. Each of these variables must be included in future analysis if an I48N forecasting system is to be developed. Each of these variables should be tested at 0-3-year

lags, in order to better understand at which, point in the transit of an iceberg these variables are most impactful. These data can be analyzed in largely the same method as outlined in this work, with the addition of including all of these new variables in a multiple linear regression, to more precisely identify how much variance in the number of I48Ns can be attributed to each. This step would be tremendously useful in better understanding the gaps in variance left by the variables tested in this work.

In order to analyze these variables most strongly, an approach utilizing remotely sensed satellite imagery, as well as spatial analysis. In addition to the aforementioned variables, the Case studies reveal some additional variables of interest, including Sea Level Pressure, and Geopotential Height as new variables. While these variables are related to each other, they also related directly to Arctic Teleconnections. Examining these variables individually, and with respect to teleconnections can yield new information regarding atmospheric setup that leads to iceberg years of varying intensity.

Expanded statistical analysis includes both the use of improved and broadened datasets, as well as inclusion of strong spatial analysis methods. While sea ice is explored in this work, expanding the spatial boundaries of the area to include the entire Labrador shelf for further regression testing. Additionally, spatial sea ice data for Labrador Sea, Davis Strait and Baffin Bay may be used to produce hotspot analysis of where Ice is thickest or most concentrated in and before ice years with high and low number of Icebergs. This analysis could be crucial addition to future forecasting methods. The same method can be used for spatial SST data to identify where and when warm and cold seas are most impactful to the survival of I48Ns.

With the larger picture quantified and analyzed by the previous suggested steps, the final category regard in-situ study. There is a need to observe the transit of I48Ns in-situ. This in situ method would build upon the GPS Iceberg tracking studies developed by Robe (1982), Hansen and Hartmann (1998), and Larsen and others (2016), in which large icebergs are identified and measured in source glaciers on Greenland's West coast and are fit with a GPS Transponder to measure location and speed. Larsen and other (2016) most recently conducted this method in 2011, however were limited by transponder battery life, and collected data for a maximum of 148 days. Repeating this method with transponders capable of reporting data for 3+ years would be ideal and would allow for complex spatial analysis of the factors that impact I48N transit. This undertaking coupled with the statistically significant lags determined in this work would allow an insight into iceberg transit into the North Atlantic so far undetermined.

### **6.3 Concluding Statement**

As the climate continues to change, and North Atlantic trade expands, it is essential to develop a reliable iceberg forecasting system. This work is a first step on a path to making such a method a reality. The International Ice Patrol's mission to observe and record Icebergs in the North Atlantic and make reports available for mariners remains as essential to safety at sea as it did when the IIP was founded in 1914. Creating a forecasting system is of great importance to the IIP, and understanding the climatic, meteorological, and oceanographic drivers of North Atlantic Icebergs will allow this product to be created.

The key findings of this work, and the future directions established by the statistical analysis and case studies, leads in a direction that will make forecasting North Atlantic Icebergs a reality.

## APPENDIX I

### Monthly Iceberg Counts 1983-2020 (G10028)

Year	Oct	Nov	Dec	Jan	Feb	Mar	Apr	May	Jun	Jul	Aug	Sep	Total
1983	0	0	2	9	165	124	339	465	168	76	4	0	1352
1984	0	0	0	0	0	101	953	484	227	335	93	9	2202
1985	3	11	7	2	57	129	208	205	247	123	39	32	1063
1986	0	0	0	0	3	40	60	59	24	18	0	0	204
1987	0	0	5	2	14	48	76	29	127	15	2	0	318
1988	0	0	0	0	0	8	95	33	20	19	10	2	187
1989	3	0	0	0	19	127	68	39	35	10	0	0	301
1990	0	0	0	0	9	112	376	187	76	26	7	0	793
1991	0	0	0	0	20	115	144	269	1030	325	71	0	1974
1992	0	0	0	0	69	53	99	230	103	171	132	19	876
1993	0	0	16	112	336	276	428	338	188	50	8	1	1753
1994	0	0	0	0	79	529	208	377	387	161	24	0	1765
1995	0	0	0	0	43	385	334	405	218	41	6	0	1432
1996	0	0	0	0	0	4	297	187	108	14	1	0	611
1997	0	0	0	0	10	475	162	238	80	43	3	0	1011
1998	0	0	0	0	5	26	70	1017	247	15	0	0	1380
1999	0	0	0	0	0	1	2	11	5	3	0	0	22
2000	0	0	0	0	0	286	239	212	65	41	0	0	843
2001	0	0	0	0	4	31	31	19	4	0	0	0	89
2002	0	0	0	0	16	173	316	308	64	0	0	0	877
2003	0	0	0	0	0	84	263	494	76	10	0	0	927
2004	0	0	0	0	0	0	24	114	117	7	0	0	262
2005	0	0	0	0	0	9	1	1	0	0	0	0	11
2006	0	0	0	0	0	0	0	0	0	0	0	0	0
2007	0	0	0	0	0	4	40	71	183	26	0	0	324
2008	0	0	0	0	0	45	712	173	43	3	0	0	976
2009	0	0	0	0	0	286	266	450	180	21	1	0	1204
2010	0	0	0	0	0	0	0	0	1	0	0	0	1
2011	0	0	0	0	0	0	0	3	0	0	0	0	3
2012	0	0	0	0	0	93	136	256	14	0	0	0	499
2013	0	0	0	0	0	4	8	1	0	0	0	0	13
2014	0	0	0	0	15	268	541	532	172	16	2	0	1546
2015	2	2	0	0	0	106	485	240	240	77	13	0	1165
2016	0	0	0	4	26	182	159	199	91	25	1	0	687
2017	0	0	0	0	11	282	383	206	99	16	7	4	1008
2018	0	0	0	0	3	55	41	47	61	0	1	0	208
2019	0	0	0	0	15	390	274	792	44	0	0	0	1515
2020	0	0	0	0	1	41	33	76	17	1	0	0	169

**APPENDIX II**

**Logistic Regression Binary Variables**

<b>Year</b>	<b>Tele. Indices</b>		<b>Iceberg Category Binary Variable</b>				<b>Category</b>
	<b>NAOI</b>	<b>AOI</b>	<b>Light</b>	<b>Moderate</b>	<b>Heavy</b>	<b>Extreme</b>	
<b>1983</b>	0.683636	0.07775	0	0	1	0	3
<b>1984</b>	0.262727	-0.05358	0	0	0	1	4
<b>1985</b>	-0.20545	-0.40742	0	0	1	0	3
<b>1986</b>	0.252727	-0.29367	1	0	0	0	1
<b>1987</b>	0.358182	-0.24742	0	1	0	0	2
<b>1988</b>	0.207273	-0.19525	1	0	0	0	1
<b>1989</b>	0.598182	1.057917	0	1	0	0	2
<b>1990</b>	0.44	0.851167	0	1	0	0	2
<b>1991</b>	0.2	0.264667	0	0	0	1	4
<b>1992</b>	0.750909	0.408833	0	1	0	0	2
<b>1993</b>	-0.07182	0.216167	0	0	0	1	4
<b>1994</b>	0.904545	0.322917	0	0	0	1	4
<b>1995</b>	0.297273	0.193917	0	0	0	1	4
<b>1996</b>	-0.20636	-0.57075	0	1	0	0	2
<b>1997</b>	-0.11182	-0.03717	0	1	0	0	2
<b>1998</b>	-0.69364	-0.40683	0	0	1	0	3
<b>1999</b>	0.197273	-0.00833	1	0	0	0	1
<b>2000</b>	0.520909	0.392417	0	1	0	0	2
<b>2001</b>	-0.15273	-0.48	1	0	0	0	1
<b>2002</b>	0.375455	0.464083	0	1	0	0	2
<b>2003</b>	-0.22545	-0.24317	0	1	0	0	2
<b>2004</b>	0.175455	-0.28867	0	1	0	0	2
<b>2005</b>	-0.11545	-0.10533	1	0	0	0	1
<b>2006</b>	-0.19455	-0.16392	1	0	0	0	1
<b>2007</b>	-0.04273	0.3595	0	1	0	0	2
<b>2008</b>	-0.32273	0.032583	0	1	0	0	2
<b>2009</b>	-0.19	0.2455	0	0	1	0	3
<b>2010</b>	-1.05636	-1.12775	1	0	0	0	1
<b>2011</b>	-0.51727	-0.13717	1	0	0	0	1
<b>2012</b>	0.169091	0.473	0	1	0	0	2
<b>2013</b>	-0.06909	-0.59408	1	0	0	0	1
<b>2014</b>	-0.00727	0.3515	0	0	0	1	4
<b>2015</b>	0.245455	0.26375	0	0	1	0	3
<b>2016</b>	0.238182	0.209167	0	1	0	0	2
<b>2017</b>	0.270909	0.148333	0	1	0	0	2
<b>2018</b>	0.997273	0.298417	1	0	0	0	1
<b>2019</b>	-0.20909	-0.1195	0	0	0	1	4
<b>2020</b>	0.09	0.685917	1	0	0	0	1

## LITERATURE CITED

- Akaike, H., 1973. Information Theory and an Extension of the Maximum Likelihood Principle. *International Symposium on Information Theory*. Eds., Petrov, B.N., and F. Csaki 267-281
- Barnston, A. G., and R. E. Livezey. 1987. Classification, seasonality, and persistence of low-frequency atmospheric circulation patterns. *Monthly Weather Review.*, 115, 1083-1126.
- Barry, R., and T. Gan. 2011. *The Global Cryosphere*. Cambridge, UK. Cambridge University Press.
- Barry, R., and E. Hall-McKim. 2014. *Essentials of the Earth's Climate System*. Cambridge, UK. Cambridge University Press.
- Bevis, M., C. Harig, S. A. Khan, A. Brown, F.J. Simons, M. Willis, X. Fettweis, M.R. van den Broeke, F.B Madsen, E. Kendrick, D.J. Caccamise, T. van Dam, P. Knudsen, and T. Nylen. 2019. Accelerating changes in ice mass within Greenland, and the Ice Sheet's sensitivity to atmospheric forcing. *Proceedings of the National Academy of Sciences*, 116(6), 1934–1939. doi:10.1073/pnas.1806562116
- Bigg, G.R. 1999. An estimate of the flux of iceberg calving from Greenland. *Arctic, Antarctic, and Alpine Research* 31, 174–178. doi:10.2307/1552605
- . 2015. *Icebergs. Their Science and Links to Global Change*. Cambridge, UK. Cambridge University Press
- Bigg, G. R, H.L. Wei, D.J. Wilton, Y Zhao, S.A. Billings, E. Hanna, V. Kadiramanathan. 2014. A century of variation in the dependence of Greenland iceberg calving on ice sheet surface mass balance and regional climate change. *Proceedings of the Royal Society, A*. 470: 20130662. doi:10.1098/rspa.2013.0662

- Burnham, K.P., and D.R. Anderson. 2002. *Model Selection and Multimodal Inference: A Practical Information-Theoretic Approach*. New York, NY, Springer
- Box, J. E., X. Fettweis, J.C Stroeve, M. Tedesco, D.K. Hall, and K. Steffen. 2012. Greenland Ice Sheet Albedo Feedback: Thermodynamics and Atmospheric Drivers. *The Cryosphere*, 6(4), 821–839. doi:10.5194/tc-6-821-2012
- Delworth, T.L, and M.E. Mann. 2000. "Observed and simulated multidecadal variability in the Northern Hemisphere", *Climate Dynamics*. 16: 661-676.
- Dussin, R., B. Barnier, L. Brodeau, & J.M. Molines. 2016. *The making of the DRAKKAR FORCING SET DFS5*. DRAKKAR/MyOcean Report 01-14-16. Grenoble, FR
- Ellsworth, L., and E.H. Smith. 1932. Report of the Preliminary Results of the Aeroarctic Expedition with “Graf Zeppelin”, 1931. *Geographical Review*. 22(1)- 61-82
- Fenty, I., and P. Heimbach. 2013. *Journal of Physical Oceanography* 43(5): 884-904
- Fischer, J., M. Visbeck, R. Zantopp, and N. Nunes. 2010. Interannual to decadal variability of outflow from the Labrador Sea. *Geophysical Research Letters*, 37. L24610, doi:10.1029/2010GL045321
- FitzMaurice, A., F. Straneo, C. Cenedese, & M. Andres. 2016. Effect of sheared flow on iceberg motion and melting. *Geophysical Research Letters*.
- FitzMaurice, A., C. Cenedese and F. Straneo. 2017. Nonlinear response of iceberg side melting to ocean currents. *Geophysical Research Letters*.
- Francis, J., and S.T. Vavrus. 2012. Evidence linking arctic amplification to extreme weather in Mid-Latitudes. *Geophysical Research Letters*. 36(9): L06801
- . 2015. Evidence for a wavier jet stream in response to rapid Arctic warming. *Environmental Research Letters*. 10(1) 014005

- Greenan, B.J.W, and S.J. Prisenberg. 1998. Wind Forcing of Ice Cover in Labrador Shelf Marginal Ice Zone. *Atmosphere-Ocean* 36(2): 71-93
- Hanafin, J. A., 2002: *On sea surface properties and characteristics in the infrared*. Ph.D., Meteorology and Physical Oceanography, University of Miami
- Hansen, KQ and Hartmann, H. 1998 Berg Watch 97: iceberg drift data and satellite imagery in eastern Baffin Bay. *Danish Meteorological Institute Technical Report* 97-10
- Holton, J, 1992 *An Introduction to Dynamic Meteorology* San Diego, California; Academic Press.
- Howat, I.M., J.E. Box, Y. Ahn, A. Herrington, E.M. McFadden. 2010. Seasonal variability in the dynamics of marine-terminating outlet glaciers in Greenland. *Journal of Glaciology* 56, 601–613.
- Hurrell, J.W. 1995. Decadal trends in the North Atlantic Oscillation and relationships to regional temperature and precipitation. *Science* 269, 676-679.
- Hurrell, J. W. 2020. *The Climate Data Guide: Hurrell North Atlantic Oscillation (NAO) Index (pc based)*. UCAR. Boulder, CO <https://climatedataguide.ucar.edu/climate-data/hurrell-north-atlantic-oscillation-nao-index-pc-based>
- Huggett, R. J. 2010. *Physical geography: The key concepts*. New York, NY. Routledge.
- International Ice Patrol. 1994. Report of the International Ice Patrol in the North Atlantic 1994 Season. Bulletin No. 80 CG-188-49. Alexandria, VA: U.S. Coast Guard.
- 1995. *International Ice Patrol (IIP) Iceberg Sightings Database, Version 1*. Boulder, Colorado USA. NSIDC: National Snow and Ice Data Center.
- 2011. Report of the International Ice Patrol in the North Atlantic 2011 Season. Bulletin No. 97 CG-188-66. Alexandria, VA: U.S. Coast Guard.
- 2014. Report of the International Ice Patrol in the North Atlantic 2014 Season. Bulletin No. 100 CG-188-69. Alexandria, VA: U.S. Coast Guard.

- . 2016. Report of the International Ice Patrol in the North Atlantic 2016 Season. Bulletin No. 102 CG-188-70. Alexandria, VA: U.S. Coast Guard.
- . 2018. Report of the International Ice Patrol in the North Atlantic 2018 Season. Bulletin No. 104 CG-188-73. Alexandria, VA: U.S. Coast Guard.
- . 2020. International Ice Patrol Annual Count of Icebergs South of 48 Degrees North, 1900 to Present, Version 1. doi: /10.7265/z6e8-3027.
- Jones, P.D., T. Jónsson. and D. Wheeler. 1997. Extension to the North Atlantic Oscillation using early instrumental pressure observations from Gibraltar and South-West Iceland. *International Journal of Climatology* 17, 1433-1450.
- Kalnay, E., M. Kanamitsu, R. Kistler, W. Collins, D. Deaven, L. Gandin, M. Iredell, S. Saha, G. White, J. Woolen et al. 1996. The NCEP/NCAR 40- Year Reanalysis Project. *Bulletin of the American Meteorological Society*, 77, 437-471.
- Kanamitsu, M., W. Ebisuzaki, J. Woolen, S. Yang, J.J. Hnilo, M. Fiorino and G.L. Potter. 2002: NCEP-DOE AMIP-II Reanalysis (R-2), *Bulletin of the American Meteorological Society*, 83, 1631-1643.
- Kistler, R., E. Kalnay, W. Collins, S. Saha, G. White, J. Woolen, M. Chelliah, W. Ebisuzaki, M Kanamitsu, V. Kousky et al., 2001: The NCEP-NCAR 50-Year Reanalysis: Monthly means CD-ROM and documentation. *Bulletin of the American Meteorological Society*, 82,247-267.
- Lamb, P. J., and R.A. Pepler. 1987. North Atlantic Oscillation: concept and an application. *Bulletin of the American Meteorological Society*. 68 1218–1225
- Katsaros, K. B., W. T. Liu, J. A. Businger, and J. E. Tillman, 1977: Heat transport and thermal structure in the interfacial boundary layer measured in an open tank. *Journal of Fluid Mechanics*, 83: 311-335.

- Larsen, P., Hansen, M., Buus-Hinkler, J., Krane, K., & Sønderkov, C. (2016). Field tracking (GPS) of ten icebergs in eastern Baffin Bay, offshore Upernavik, northwest Greenland. *Journal of Glaciology*, 61(227), 421-437.
- Maier, N., N. Humphrey, J. Harper & T. Meierbachtol. 2019. Sliding dominates slow-flowing margin regions, Greenland Ice Sheet. *Science Advances* 5(7)
- Mann, M.E., J. Park, and R.S. Bradley. 1995 "Global interdecadal and century-scale climate oscillations during the past five centuries", *Nature*. 378, 266-270, doi:10.1038/378266a0
- Mann, M. E., B.A. Steinman, D.J. Brouillette, & S.K. Miller. 2021. Multidecadal climate oscillations during the Past millennium driven by volcanic forcing. *Science*, 371(6533), 1014–1019.
- Marko J.R, D.B. Fissel, P. Wadhams, P.M Kelly and R.D Brown. 1994. Iceberg severity off eastern North America, its relationship to sea ice variability and climatic change. *Journal of Climate*. 7, 1335–1351
- Meyers, L.S., G. Gamst, A.J. Guarino, 2013 “*Applied Multivariate Research: Design and Interpretation, 2<sup>nd</sup> Edition*” Thousand Oaks, CA: SAGE
- Murphy D.L., and J.L Cass. 2012. The international Ice Patrol – Safeguarding life and property at sea. *Coast Guard Maritime Safety Security Council*. 69, 13-16
- National Weather Service. 2009. *National Weather Service Glossary*. Silver Spring, MD. <https://w1.weather.gov/glossary/> (last accessed July 7, 2022)
- Palter, J.B., C.-A Caron, K.L. Law, J.K. Willis, D.S. Trossman, I.M Yashayaev, and D. Gilbert, 2016. Variability of the directly observed, middepth subpolar North Atlantic circulation. *Geophysical Research Letters* 42.
- Paterson, W.S.B. 1994. *The Physics of Glaciers*. Oxford, UK. Elsevier

- Rignot, E., Koppes, M., & Velicogna, I. (2010). Rapid submarine melting of the calving faces of West Greenland glaciers. *Nature Geoscience*, 3, 187–191.
- Rignot, E., Koppes, M., & Velicogna, I. (2010). Rapid submarine melting of the calving faces of West Greenland glaciers. *Nature Geoscience*, 3, 187–191.
- Rignot, E., M. Koppes, and I. Velicogna. 2010. Rapid submarine melting of the calving faces of West Greenland glaciers. *Nature Geosciences*, 3, 187-191
- Rignot, E., I. Fenty, Y. Xu, C. Cai, and C. Kemp. 2015. Undercutting of marine-terminating glaciers in West Greenland. *Geophysical Research Letters*, 42(14), 5909–5917.  
doi:10.1002/2015gl064236
- Robe, R.Q. (1982) *Iceberg drift near Greenland, 1980 to 1982*. United States Coast Guard Research and Development Center, Groton
- Rudnickas, D., and K. Serumgard. 2018. “*Appendix B. Updated Iceberg Season Severity Definitions: Trends and Standardization*” in Report of the International Ice Patrol in the North Atlantic Bulletin No. 104 CG188-73.
- Serreze, M., and R. Barry. 2014 *The Arctic Climate System*. Cambridge University Press
- Smith, E.H. 1926 Oceanography of the Ice Patrol *Transactions American Physical Union* 7(1): 106-112
- Thompson, D.W.J., and J.M. Wallace 1998: The Arctic Oscillation signature in wintertime geopotential height and temperature fields. *Geophysical Research Letters* 25, 1297-1300.
- Thompson, D. W. J., and J. M. Wallace, 2000: Annular modes in the extratropical circulation. Part I: Month-to-month variability. *Journal of Climate*, 13, 1000-1016.
- Trivers, G. 1994. *International Ice Patrol's Iceberg Season Severity*. Report of the International Ice Patrol Services in the North Atlantic Bulletin No. 80, Appendix C, pp 49-59.

- van den Broeke, M., J. Bamber, J. Ettema, E. Rignot, E. Schrama, W.J van de Berg, E. van Meijgaard, I. Velicogna, & B. Wouters 2009. Partitioning recent greenland mass loss. *Science*, 326(5955), 984–986.
- Walker, G.T. 1924 Correlation in Seasonal Variations of Weather, IX. A Further Study of World Weather, *Memoirs of the India Meteorological Department* 24(9), 275-333.
- . 1928. World Weather, *Quarterly Journal of the Royal Meteorological Society*, 54 (226), 79-87
- Walker, G.T. and E.W. Bliss. 1932. World Weather V, *Memoirs of the Royal Meteorological Society*, 4, 53-84
- . World Weather VI, *Memoirs of the Royal Meteorological Society*, 4, (39), 119-139.
- Wallace and D. S. Gutzler, 1981: Teleconnections in the geopotential height field during the Northern Hemisphere winter. *Monthly Weather Review*, 109, 784-812.
- Wheeler, E. P. 1914. International conference on the safety of life at sea. *Nature*, 92(2309), 616–617.
- Wood, M., E. Rignot, I. Fenty, D. Menemenlis, R. Millan, M. Morlighem, J. Mouginot, and H. Seroussi. 2018. Ocean-Induced melt Triggers glacier retreat in Northwest Greenland. *Geophysical Research Letters*, 45(16), 8334–8342.
- Yang, Y., Y. Zhang, X. San Liang, Q. Cheng, J. Tsou. 2021. Evolution of Arctic Ocean Surface Circulation from 1958 to 2017. *Global and Planetary Change*. 206, 103638.
- Yashayaev I. 2007. Hydrographic changes in the Labrador Sea, 1960–2005. *Progress in Oceanography*. 73, 242–276.

Zhao, Y., G.R. Bigg, S.A Billings, E. Hanna, A.J. Sole, H. Wei, V. Kadiramanathan, & D.J. Wilton. 2016. Inferring the variation of climatic and glaciological contributions to West Greenland iceberg discharge in the Twentieth Century. *Cold Regions Science Technology*. 121, 167-178